Synthesis of Novel Zinc Anode via Electroplating for Rechargeable Hybrid Aqueous Batteries

by

Kyung Eun Kate Sun

A thesis

presented to the University of Waterloo

in fulfillment of the

thesis requirement for the degree of

Mater of Applied Science

in

Chemical Engineering

Waterloo, Ontario, Canada, 2016

© Kyung Eun Kate Sun 2016

AUTHOR'S DECLARATION

I hereby declare that I am the sole author of this thesis. This is a true copy of the thesis, including any required final revisions, as accepted by my examiners.

I understand that my thesis may be made electronically available to the public.

ABSTRACT

With the rise of the environmental concerns from combustion of fossil fuels, the demand for the alternative clean energy sources has increased. One of the alternatives is rechargeable batteries. Among many types of rechargeable batteries, lithium-ion batteries have been the most promising due to the high energy density and long lifespan. The current lithium-ion batteries, however, hold a drawback as they utilize organic electrolytes. The use of organic electrolytes not only raises safety and environmental concerns, but also results in a higher manufacturing cost than would be with aqueous electrolytes. Therefore, these issues can be solved by replacing the organic electrolytes with aqueous electrolytes. Among the many types of lithium-ion batteries with aqueous electrolytes, Rechargeable Hybrid Aqueous Battery (ReHAB) was selected in this project.

ReHAB utilizes lithium manganese oxide ($LiMn_2O_4$) as the cathode and zinc as the anode. $LiMn_2O_4$ is a good candidate because tightly bounded lithium ions make $LiMn_2O_4$ stable in air and water. Also, it shows a small volume variation between lithiated and non-lithiated states. Zinc metal was chosen because of its low redox potential, good reversibility, high over-potential for hydrogen evolution in acidic environment, large specific capacity, good corrosion resistance, and cost effectiveness.

While ReHAB is free of the problems posed by organic electrolytes in traditional Li-ion batteries, the current ReHAB technology must be improved to perform competitively in market. More specifically regarding the zinc anode, there are issues of corrosion, dendrite formation, and hydrogen evolution. Therefore, the goal of this project was to synthesize novel zinc anodes via electroplating with additives (organic and inorganic) reported in literature to mitigate issues of corrosion, dendrite formation, and hydrogen evolution (side reactions). The selected organic additives were cetyl trimethylammonium bromide (CTAB), sodium dodecyle sulfate (SDS), polyethylene glycol 8000 (PEG), and thiourea; and the inorganic additives were indium (II) sulfate, tin (IV) oxide, and boric acid. Each anode was characterized by the following measurements to rate its performance: float current (for side reactions), corrosion current, cyclability, x-ray diffraction (for crystalline structure and indication of high/low deposition efficiency), and scanning electron microscope (for morphology).

All the anodes created with the inorganic and almost all with the organic additives performed better than the commercial zinc anode. Among the organic additives tested, Zn-SDS performed the best, with the lowest float current and corrosion current measurements and the highest retention of 79% at the end of its 1000th cycle. Among the inorganic additives tested, each fared very similarity, with similar float current and corrosion rate, and retaining in average 78% of the initial discharge capacity at the end of 1000th cycle.

Between the organic and inorganic additives, however, the XRD results suggested that in general the zinc deposition efficiencies may be lower for inorganic additives (and thus less favourable when scaling up for commercial production). If the lower current efficiency of inorganic additives (hinted by the XRD results) is verified to be true, then the organic additives that either performed

better than or as well as the inorganic additives would be the better choice for the next generation of ReHAB.

ACKNOWLEGEMENTS

DEDICATION

Dedicated to My Family

Table of Contents

List of Figures

List of Tables

List of Abbreviations, Symbols, and Nomenclature

AGM	Absorptive Glass Mat
CTAB	Cetyl Trimethylammonium Bromide
FESEM	Field Emission Scanning Electron Microscopy
I	Total Current
I_{corr}	Corrosion Current
j	Current Density
i_{corr}	Corrosion Current Density
L	Distance
NMP	1-methyl-2-pyrrolidinone
OCV	Open Circuit Voltage
PEG	Polyethylene Glycol 8000
PPM	Parts Per Million
PVDF	Polyvinylidene Fluoride
ReHAB	Rechargeable Hybrid Aqueous Battery
SHE	Standard Hydrogen Electrode
SDS	Sodium Dodecyle Sulfate
V	Voltage
V_{corr}	Corrosion Potential
XRD	X-ray Diffraction
β_a	Anodic Tafel Constant
β_c	Cathodic Tafel Constant

Chapter 1: Introduction of Thesis

1.1 Research Motivation

Since the eighteenth century, fossil fuels have been an excellent energy source in many applications. They, however, have since raised environmental concerns due to their harmful combustion wastes and fast depletion rate. The combustion products, such as carbon dioxide and sulphur dioxide, contributed to the global warming, and some have predicted that the oil and gas will deplete in less than 40 years [1]. The search for and the development of the cleaner energy sources have been – and still are – actively pursued. And out of many approaches, the area of chemical rechargeable batteries (also called secondary batteries) has garnered much interest and investment as is evident today in their ubiquitousness for their storage capacities, reduction in material waste as well as pollution/by-products.

The first battery was invented in 1800 by Volta, and in 1895, the idea and demonstration of a rechargeable battery were carried out by Gaston Planté. Since then, various types of secondary batteries have been proposed, such as nickel-cadmium, nickel-metal-hydride, and lithium-ion batteries. Among these different batteries, lithium-ion batteries have been the most promising due to the high energy density (shown in **Figure 1**) and long lifespan [2, 3].
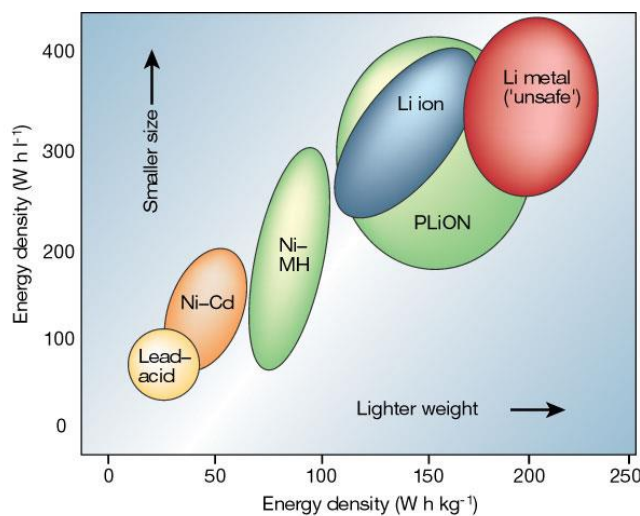
Figure 1 - *Comparison of the different battery technologies in terms of volumetric and gravimetric energy density [2]*

Despite the many advantages of traditional lithium-ion batteries, there is one major drawback – the use of organic electrolytes. With organic electrolytes, the lithium-ion batteries can be operated at a wide voltage range, but due to the flammable and toxic characteristics of the organic electrolytes, safety and environmental concerns arise with the leakage of the electrolytes [3]. Moreover, the manufacturing with organic electrolytes is complicated and expensive as they are moisture- and air- sensitive [3, 4]. Thus, the organic electrolytes can be replaced with aqueous electrolytes to solve these problems. Among different kinds of aqueous batteries, Rechargeable Hybrid Aqueous Battery (ReHAB) was selected for this report. ReHAB, as any other proposed batteries, still needs some improvements. In this report, the studies on the anode to improve the performance of ReHAB are presented.

1.2 Research Objectives

The project goal was to develop novel zinc anodes via electroplating to improve upon the current ReHAB technology operating with a commercialize zinc anode. The commercialized zinc anode in ReHAB faces many problems, such as corrosion, dendrite formation, and hydrogen evolution [5]. Therefore, the goal was to create novel anodes by employing various additives, known to mitigate the aforementioned problems, during the synthesis of the zinc anode. For this study, 7 different additives were selected: CTAB, SDS, PEG, thiourea, tin oxide, boric acid, and indium sulfate.

The crystalline structures of the zinc deposited with the additives were studied with XRD to understand how each additive modified the structure. Their morphologies were observed with SEM. To determine whether they assisted in alleviating the current zinc problems in ReHAB, the corrosion and battery tests were carried out. Lastly, to examine if these electroplated anodes could replace the commercialized zinc foil in ReHAB, the batteries were assembled with the synthesized anode and tested.

1.3 Outline of Thesis

This thesis contains 4 chapters:

Chapter 1 contains the overview and the research objectives

Chapter 2 includes the literature review on the aqueous batteries, introduction to electroplating, and fundamentals of additives

Chapter 3 presents the experimental methodologies, technique used for sample analysis, experimental data and analysis, and conclusion

Chapter 4 contains the future work

Chapter 2: Introduction to ReHAB and Problems of Anode

2.1 History of Rechargeable Aqueous Batteries

With the rise of the environmental concerns with the combustion wastes from fossil fuels, the demand for the alternative renewable energy sources has also increased. One of the cleanest energy sources is the secondary batteries. Among the many types of rechargeable batteries, lithium-ion batteries are one of the most promising batteries as they show high energy density and long lifespan. They can also operate at a wide electrochemical stability window (voltage range at which substance is stable) of 3-5V [3]. Hence, they have been used in various applications, such as portable electronics and vehicles.

Despite these advantages, there is a drawback of lithium-ion batteries due to its use of the traditional organic electrolytes. The organic electrolytes are highly toxic and flammable. Moreover, the manufacturing cost of the lithium-ion batteries is expensive due to the organic electrolytes being moisture- and air- sensitive. In order to mitigate these issues, the employment of aqueous electrolytes can be made. Although, the aqueous electrolytes show smaller electrochemical stability window in comparison to the organic electrolytes, they can guarantee safety, environmentally friendliness, and reduced manufacturing cost.

In 1994, Dahn and colleague [6] introduced the first aqueous rechargeable lithium-ion battery (ARLB), which consisted of lithium manganese oxide ($LiMn_2O_4$) as the negative electrode (or anode) and carbon rod as the positive electrode (or cathode). During the charge process, the lithium ions de-intercalated from the positive electrode (or cathode) and intercalated into the negative electrode (or anode), and vice versa during the discharge process. The authors determined that the electrodes were stable in the potential range of $2.3V \leq V(x) \leq 3.5V$ when ARLB consisted of 1M LiOH as the electrolyte [6]. The ARLB demonstrated higher operating voltage than the lead-acid battery, but poorer battery cycling performance [7, 8].

Since the invention of ARLB, other types of ARLB were also introduced. In 2007, G.J. Wang *et al*. [9] studied ARLB with lithium trivandate (LiV_3O_8) anode and $LiMn_2O_4$ cathode operating in 2M lithium sulfate electrolyte (Li_2SO_4). The authors confirmed that both of the synthesized electrodes were stable in the aqueous solution, and the batteries with these electrodes produced the

1st coulombic efficiency of 89.2%, and the retention of 53.5% after 100th cycle [9]. These results indicated the improvements of ARLB in comparison to those reported in the earlier literature.

J. Luo's group [10] studied the effect oxygen in an aqueous electrolyte in the aqueous rechargeable batteries. The battery was composed of lithium iron phosphate ($LiFePO_4$) as the cathode, lithium titanium phosphate ($LiTi_2(PO_4)_3$) as the anode, and Li_2SO_4 as the electrolyte. By removing the oxygen from the electrolyte, the batteries were able to retain over 90% of capacity until 1000 cycles [10]. With the presence of oxygen, however, the capacity of the battery faded quickly. These results demonstrated that the absence of the oxygen in the electrolyte prolonged the cyclability of the batteries due to the reduced chance of the anode reacting with the oxygen.

2.2 Rechargeable Hybrid Aqueous Batteries

Out of many types of aqueous batteries, Rechargeable Hybrid Aqueous Battery (or ReHAB) was selected for this project. ReHAB, invented in 2012 by Chen's research group, utilizes $LiMn_2O_4$ as the cathode, zinc foil as the anode, and a chloride solution containing lithium and zinc ions as the electrolyte. The combination of the cathode and the anode produces the battery voltage of ~1.8V [3]. The battery delivers the energy density of 50-80 Wh kg^{-1}, which is higher than that of the lead-acid battery (30-50 Wh kg^{-1}), the one with an aqueous electrolyte currently used in the practical applications [3]. Also, ReHAB could run up to 1000 cycles with 90% of its original capacity.

The mechanism of ReHAB is more complex as two ions – zinc as well as lithium ions – take a part during cycling of the batteries. During the charge process, lithium ions are de-intercalated from the cathode as shown in the following reaction:

$$LiMn_2O_4 \rightarrow Li_{1-x}Mn_2O_4 + xLi^+ + xe^- \tag{1}$$

Simultaneously, zinc ions in the electrolyte are deposited on the anode:

$$Zn^{2+} + 2e^- \rightarrow Zn \tag{2}$$

The reverse reactions of (1) and (2) are expected during the discharge process.

If the batteries were operated ideally, the current efficiencies of chemical reaction (1) and (2) would be 100% each. But, in reality, side reactions occur along with the above two reactions. The cathodic side reaction is water electrolysis as shown below:

$$2H_2O \rightarrow 4H + O_2 \text{ (g)} + 4e^- \hspace{3cm} (3)$$
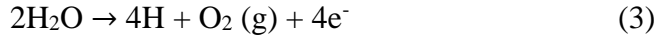
And at the anode, the main side reaction is the evolution of hydrogen:

$$2H^+ + 2e^- \rightarrow H_2 \text{ (g)} \hspace{3cm} (4)$$
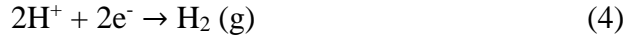
Due to these side reactions (3) and (4), the current efficiencies of the main reactions (1) and (2) are smaller than those in the ideal situation. With the smaller current efficiencies of the main reactions, the capacity of the battery decreases, and eventually the cycle life of the battery is affected [11]. Thus, it is important to inhibit side reactions during charge and discharge of a battery in order to not only maintain a high capacity, but also prolong the battery life.

2.3 Zinc Anode in Rechargeable Hybrid Aqueous Batteries

In aqueous batteries, various types of metals can be selected as the anode, such as aluminum [12], iron [13], magnesium [14], or zinc [3, 14]. Among these different metals, zinc is the most suitable to be used in aqueous-base electrolyte batteries due to its low redox potential, good reversibility, high over-potential for hydrogen evolution in acidic environment, large specific capacity, good corrosion resistance, and cost effectiveness [3, 14, 15]. Hence, many aqueous batteries, especially alkaline batteries, utilize zinc metal as the anode.

Even though there are a number of advantages of using zinc metal in aqueous batteries, zinc battery has not been commercialized due to several limitations mainly from the electrodes. On the anode side, the problems need to be solved are: metal corrosion, dendrite formation, and hydrogen gas (H_2) evolution [5, 16]. Each will be described below in more detail.

Metal corrosion contributes to the capacity decreasing overtime. The corrosion on the metal surface leads to the loss of active metal surface for electrochemical reactions. With the faster corrosion rate, the battery will lose its capacity at a faster rate, and eventually fail [16]. Moreover, the corrosion rate depends on the surface area of a sample. As well, since the corrosion of a metal is coupled with the hydrogen gas evolution, suppression of hydrogen gas also suppresses corrosion.

Another contribution to the failure of the battery is the formation of the dendrites, which decreases its coulombic efficiency [17, 18]. A dendrite is formed due to uneven zinc ion deposition. As this unbalanced zinc deposition continues, the dendrite starts to grow at the region of high deposition,

and eventually reaches the other side of the electrode, creating a short-circuit [19]. Short-circuits in batteries result overheating, fire, and in extreme cases, explosions [20].

H_2 gas is generated as a part of the side reactions. In theory, all of the electrons transferred from the anode to the cathode during zinc metal oxidation should all be consumed in the main reactions. In reality, however, some of the electrons are spent in the side reactions (producing H_2 gas), which leads to lower coulombic efficiency and evaporation of the electrolytes. As a result, the battery will lose its capacity. Therefore, the modification of zinc is necessary to mitigate these problems to enhance the performance of the zinc aqueous batteries.

Many ideas have been proposed and verified in modifying zinc electrode, such as with additives or other metals.

In 2013, S. Lee *et al*. [21] investigated the effect of the additives (Al_2O_3, Bi_2O_3, and In_2O_3) on the zinc electrode in the zinc-air batteries. The authors prepared a physical mixture of zinc powder and the additives. With these electrodes, less hydrogen gas and smaller corrosion current were observed. Among three additives, zinc powders with aluminum oxide showed the lowest hydrogen gas evolution and corrosion current. [21].

Aside from the usage of additives, alloying is another method to modify the zinc anode to prevent the aforementioned problems. C.W. Lee *et al*. [22] studied the effects of zinc alloy in the zinc-air batteries. When the alloy was composed of 90% zinc, 2.5% nickel, and 7.5% indium, the hydrogen overpotential was shifted to -2.009V, and when it contained 90% zinc, 7.5% nickel, and 2.5% indium, the overpotential shifted to -1.725V [22]. These overpotentials were more negative than that with the pure zinc of -1.609V [22]. In conclusion, the alloy with 90% zinc, 7.5% nickel, and 2.5% indium showed good reversibility and the lowest corrosion current.

Yet another method to inhibit the H_2 evolution is to coat the zinc particles with other metals. Y. Cho *et al*.[23] coated the zinc particles with varying concentrations of lithium boron oxide (LBO) by a solution process method. When zinc particles were coated with 0.1 wt. % LBO, it produced the least hydrogen gas – the indication of the lowest corrosion rate. Moreover, it also enhanced the discharge capacity from 1.57Ah (obtained from untreated zinc electrode) to 1.7Ah [23].

Finally, dendrite formation are shown to be inhibited by additives [24]. J. Kan *et al.* [18] studied the effect of Pb^{2+}, sodium lauryl sulfate, and Triton X-100 on zinc-polyaniline batteries. Each

additive was added to an electrolyte 2.5M $ZnCl_2$ + 2M NH_4Cl_2. The results showed that the addition of Triton X-100 created the most smooth zinc surface, and prolonged cycle life from 23 (battery without any additives) to 79 cycles [18].

2.3.1 Behaviour of Zinc Metal in Various Environments

In order to enhance the performance of zinc-based batteries, understanding the behaviour of zinc in different environments is an asset. There are four main factors affecting the behaviour of zinc in aqueous solutions: the pH [3], types of ions in the solution [25], oxygen concentrations [26], and the temperature [25] of the solution.

2.3.1.1 Effect of Ph

PH of the electrolytes influences the behaviour of zinc. **Figure 2** is the Pourbaix (or E_{pH}) diagram of zinc at room temperature. A Pourbaix diagram shows the oxidation products of a metal – in this case, of zinc metal – at specific environments the metal is subjected to [27]. From the oxidation products shown in the diagram, the state of the metal (stable or oxidized) is determined. For example, Zn^{2+} on the diagram represents the oxidation of zinc (or zinc corrosion). The Pourbaix diagram also indicates hydrogen and oxygen evolution regions with the slanted dotted lines *a* and *b* in **Figure 2**. Below line *a*, hydrogen is produced and above line *b*, the oxygen. Between lines *a* and *b*, water (H_2O) is generated. The slanted lines indicate that the equilibrium potential decreases with increasing pH.
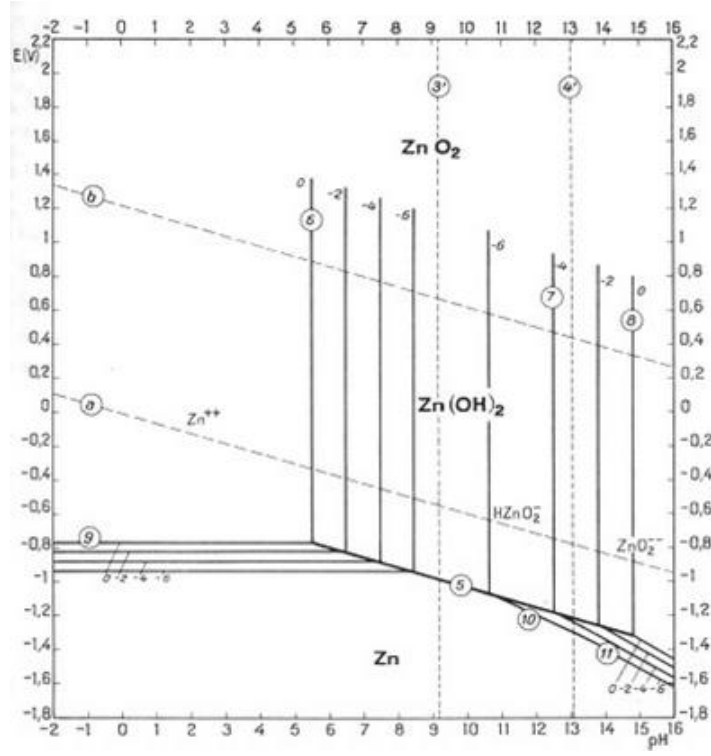
Figure 2 - *Pourbaix (E_{pH}) diagram of zinc in water at 25°C [28]*

When pH is reduced, zinc becomes oxidized to zinc ions according to **Figure 2** as follows:

$$Zn \rightarrow Zn^{2+} + 2e^- \tag{5}$$

This zinc oxidation reaction also represents the zinc corrosion. The corresponding cathodic reaction is the evolution of hydrogen gas:

$$2H^+ + 2e^- \rightarrow H_2 \text{ (g)} \tag{6}$$

This process occurs spontaneously when zinc is exposed to an acidic medium. As well, H_2 evolution is also side reaction. In other words, whether the battery with an acidic electrolyte is in operation or idle, the generation of hydrogen gas is unavoidable. Recall that hydrogen evolution is undesirable as it leads to reduction of current efficiency and evaporation of the aqueous electrolyte. Therefore, the battery will fail to operate if the current efficiency constantly falls.

However, the Pourbaix diagram also shows at a potential below -1V, zinc is immune to corrosion even in acidic solution. Therefore, it is important to find an optimal environment condition for zinc if the electrolyte in the battery is acidic.

9

In fact, J. Yan *et al.* [3] has determined the suitable acidic environment in which zinc should operate. The authors showed that when the battery consisted of $LiMn_2O_4$ as the cathode active material and zinc as the anode, the battery was able to operate at a wide range of electrochemistry window as shown in **Figure 3**. The pH of the electrolyte, however, was kept lower than 6.8 to prevent zinc hydrolysis [3]. Including the considerations of O_2 and H_2 evolution, the solubility of electrolyte salts, and the conductivity of the electrolyte, the authors concluded that the optimal pH was 4 with an operating voltage ranges from 1.4V to 2.1V *vs.* standard hydrogen electrode (*SHE*) [3]. This battery showed impressive battery performance of 90% of capacity retention at the 1000 cycle [3].
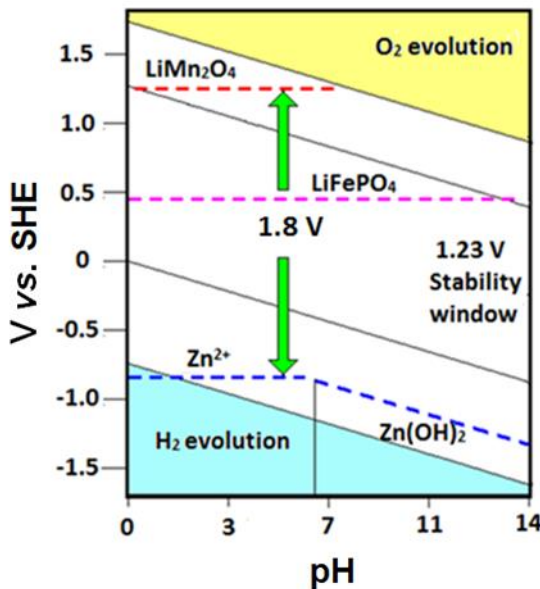
Figure 3 - *Pourbaix diagram of Zn, LiMn2O4, and LiFePO4 [3] (supplementary document)*

If the solution pH is high, oxide layers are formed on the surface of zinc due to the available hydroxide (OH^-) ions in solution, which can reduce corrosion [14, 29, 30]. In neutral and alkaline electrolytes, the products of zinc oxidation vary depending on the pH of the solution [3]:

$$Zn + 4OH^- \rightarrow [Zn(OH)_4]^{2-} + 2e^- \qquad (7)$$

or

$$Zn + 4OH^- \rightarrow ZnO_2^{2-} + 2e^- \qquad (8)$$

10

or

$$Zn + 2OH^- \rightarrow Zn(OH)_2 + 2e^- \qquad (9)$$

or

$$Zn + H_2O \rightarrow ZnO + H_2 \text{ (g)} \qquad (10)$$
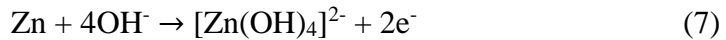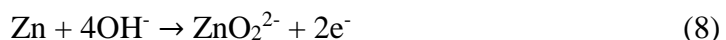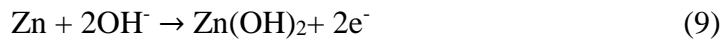
Once the oxidation products are formed during discharge, they re-dissolve back into the alkaline electrolyte as zinc is amphoteric [14, 31].

Other cases in which the oxidation products do not dissolve out, it would negatively affect the battery performance. For example, J. Zhao *et al.* [31] studied zinc anode in zinc-air batteries. Without any treatments on the zinc anode, the batteries only lasted 180 cycles, whereas the batteries with the zinc anode with MoO_3 additive (zinc-MoO_3) prolonged the cycle life up to 360 cycles [31]. This was due to the passivated film formed on the surface of the additive-free zinc anode. The zinc-MoO_3 anode, on the other hand, was less likely to passivate, producing a better cycle life in the alkaline batteries.

2.3.1.2 Effect of Solution/Electrolyte

Aside from the pH of the electrolyte or solution, the types of electrolyte used also influences the behaviour of zinc. If the solution contains ions that enhance the corrosion rate of a metal, the metal is likely to corrode faster.

D.J. Hubbard *et al.* [25] studied the effect of chloride and nitride baths on the corrosion of zinc metals [25]. In the chloride bath, increasing loss of the oxide layer and reduction in potential were observed with increasing chloride concentration – therefore, the corrosion rate was increased due to the loss of the oxide layer. In the nitride bath, however, the oxide layer was not affected and a steady-state potential was obtained; thus, the corrosion of zinc was not greatly influenced by the nitride ions. Hence, zinc was more vulnerable to corrode in the presence of chloride ions than that in the nitride ions.

In an alkaline electrolyte, the corrosion of zinc is influenced by the products created during zinc dissolution [29]. The zinc corrosion potential in KOH electrolyte, for example, can be determined from the partial oxidation of zinc and the reduction reactions as shown below [29]:

$$Zn + 4OH^- \rightarrow [Zn(OH)_4]^{2-} + 2e^- \tag{11}$$

$$2H_2O + 2e^- \rightarrow H_2 + 2OH^- \tag{12}$$
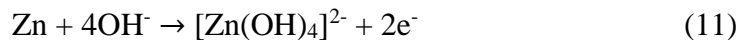
B. Szczesniak *et al.* [29] investigated the corrosion of zinc sheets in the solutions containing different salts: $ZnCl_2$ (pH = 3.75), $ZnCl_2$ + NH_4Cl, NH_4Cl, and KOH [29]. The corrosion of the zinc sheet was determined by measuring the hydrogen evolution rate. When the zinc sheet was exposed to KOH, the highest hydrogen evolution rate was achieved, and the lowest in the $ZnCl_2$ bath. This means that higher zinc corrosion was observed when it was in the KOH solution, than in the $ZnCl_2$ solution. Hence, higher zinc corrosion occurred in alkaline solutions than in acidic solutions.

2.3.1.3 Effect of Oxygen Concentration and Temperature of Solution/Electrolyte

The oxygen content and temperature of the electrolyte also play important roles on the zinc behaviour. The oxygen concentration in the solution also affects the corrosion. Depending on the state of the zinc metal, the oxidation reaction of zinc metal reacting with oxygen can be found as:

$$Zn\ (s) + \tfrac{1}{2}\ O_2\ (g) \rightarrow\ ZnO\ (s) \tag{13}$$

$$Zn\ (l) + \tfrac{1}{2}\ O_2\ (g) \rightarrow ZnO\ (s) \tag{14}$$
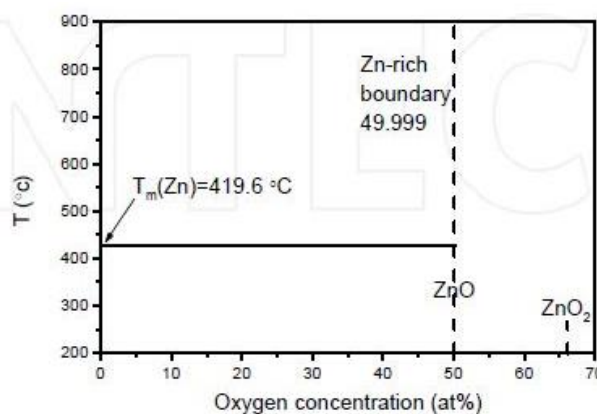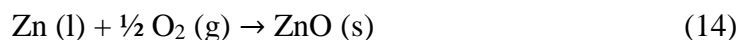
Figure 4 - Phase diagram of zinc-oxide at the different temperatures [26]

Figure 4 is the phase diagram of zinc oxide at various oxygen concentrations over a range of temperature. Above the Zn-rich boundary or at 50% of oxygen, the zinc metal or liquid zinc (if temperature is above 419.6°C) becomes zinc oxide [26]. If the oxygen concentration is over 65%, ZnO_2 is created. Since the melting point of zinc is relatively high, these are stable for a wide range of temperatures in a battery.

D.J. Hubbard *et al.* [25] studied the effect of O_2 concentration in the electrolyte on zinc corrosion by recording the steady-state potential of zinc in oxygen-concentrated and deoxygenated electrolyte (no oxygen). The results showed that the potential of zinc in the deoxygenated electrolyte was smaller than that in the oxygenated electrolyte. This represented that the zinc was more likely to corrode in the oxygenated electrolyte than that in the deoxygenated electrolyte.

Temperature also plays an important role on zinc corrosion. The same authors [25] also studied the effect of temperature on zinc corrosion in the oxygen concentrated aqueous electrolytes by placing zinc in baths at 40°C and 80°C. At the lower temperature, higher corrosion potential was observed due to the presence of zinc hydroxide and zinc oxide at lower temperature. At higher temperature, the hydroxides was converted to zinc oxide, forming a protective layer at 80°C. Therefore, the corrosion rate of the zinc was reduced at a higher temperature.

2.4 Synthesis of Zinc Anode

In general, an anode is defined as a good electrode if consistent composition, stability in the electrolyte, and good electrochemical performances are achieved [14]. Many methods to improve the performance of zinc in the aqueous batteries are proposed, such as the usage of zinc alloy powders, the synthesis of fibre or gel formed zinc, the addition of polymer additives to zinc or the battery electrolyte [32]. In order to create an anode meeting the criteria in this project, the electroplating with additives was chosen to synthesize the desired zinc anode for ReHAB.

2.4.1 Electroplating

Electroplating is a process to deposit metal cations in electroplating solution onto a desired electrode by introducing electrical current into the system. Electroplating was first invented and demonstrated in 1805 by Luigi Brugnatelli, who used a voltaic pile to electroplate gold [33]. Since its conception, it has gained a great attention not only among researchers, but also in industries for various purposes, such as the production of corrosion-resistance coatings and removal of metal ions in wastewater [34, 35].

Electroplating has attracted attention for its advantages of cost-effectiveness and simple experimental set-ups [36, 37]. Moreover, the structure, property, as well as the thickness of the deposited system can be controlled by controlling the experimental conditions since many factors influence the growth of the deposits [36]. Some of these factors are temperature [38], pH [39], current density [39], concentrations of ions present in electrolyte [40, 41], additives [42], and substrates [43]. For instance, the electroplated deposits may show smaller grain size, an increase in hardness, and a decrease in ductility with higher current density [44]. Therefore, an optimization of many factors is required to produce the optimal structure and properties for application of interest.

Various electrodeposition conditions have been studied in different types of electroplating baths, such as cyanide, zincate, or chloride [45]. High throwing power (a measure of how evenly the sample was deposited) can be obtained with a cyanide bath, but it is environmentally toxic – thus, researchers searched to replace the cyanide bath to cyanide-free bath, such as chloride and sulfate bath [46]. C. Hu *et al.* [37] compared the effect of chloride and sulfate electroplating bath. The authors concluded that the deposits from the sulfate bath showed higher dissolution efficiency than those from the chloride bath. The morphology of zinc created in the chloride bath was larger and rougher than that from the sulfate bath, indicating a higher possibility of dendrite formation.

K. Raeissi *et al.* [39] studied how the morphology and the texture of the electroplated zinc vary depending on pH and current densities. The authors observed that as the current density increased, the size of the grain decreased at pH 2, but opposite results at pH 4 (larger grain size deposited with a higher the current density). This observation due to the percentage of the basal plane (a plane perpendicular to principle axis) [39].

14

J. Hsieh *et al.* [34] studied the effect of additives that were added during zinc deposition in a chloride bath. The authors employed three different additives in the electroplating bath: (polyoxyethylene nonyl phenyl ether (NP16), o-chloro benzyl aldehyde (OCBA), and polyoxyethylene lauryl amine (S40)). Depending on the additive used, the morphology of the deposits varied. Without additives, the formation of dendrite was observed from the SEM image. The addition of one or more additives changed the dendrites into different morphologies as shown in **Figure 5** (B-E). Thus, introducing the additives into the electroplating bath modifies the morphology of the deposits.
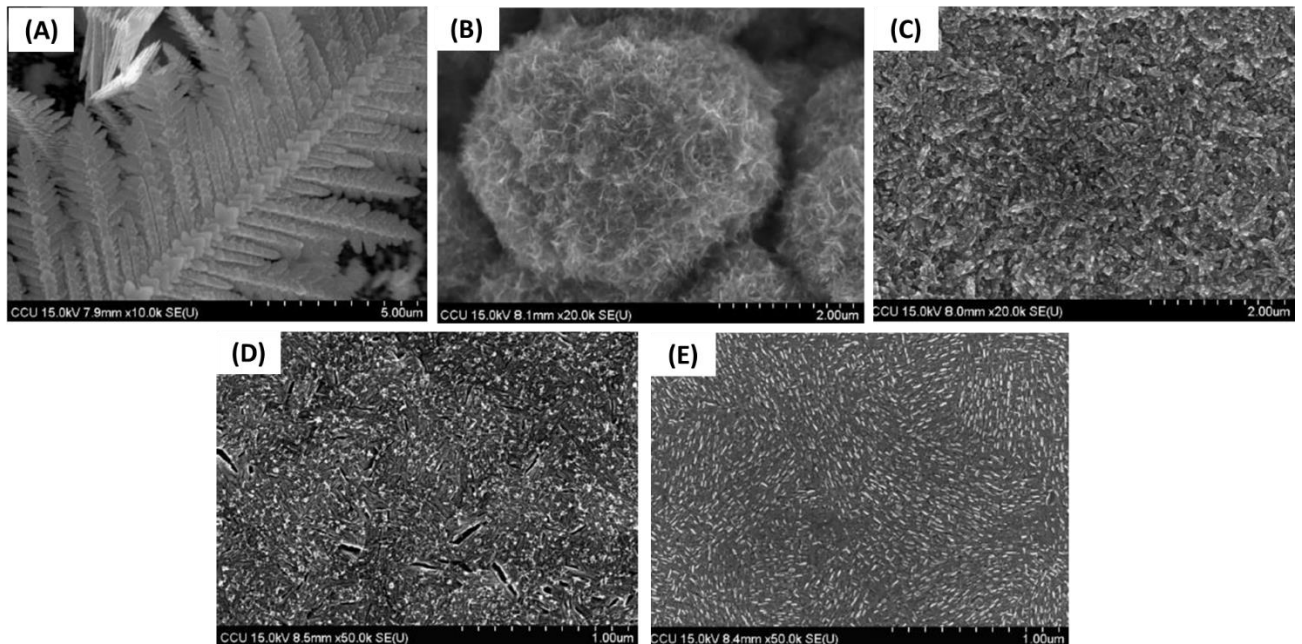
Figure 5 - Zinc plating with (A) no additive, (B) NP16, (C) NP16 and S40,
(D) NP16 and OCBA, and (D) NP16, OCBA, and S40 [34]

2.4.1 Mechanisms

An electroplating process is analogous to an electrolytic cell (reverse of galvanic cell). In a galvanic cell, metal ions from the cathode dissolve out and the same or other metal ions in solution deposit onto the anode. In electroplating, the reverse reactions occur as a current is applied to the system. The cathodic and the anodic reactions during electroplating are shown below:

$$M^{Z+} + Ze^- \rightarrow M \tag{15}$$

$$M \rightarrow M^{Z+} + Ze^- \tag{16}$$
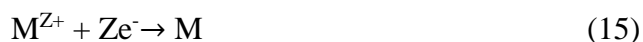
Where M^{Z+} is the metal ions dissolved in aqueous solution.

The theoretical amount of deposited metal can be calculated using Faraday's law. The actual amount, however, is less than the theoretical value due to the side reactions of hydrogen and oxygen evolution at the cathode and anode, respectively. In other words, the current efficiency, which depends on the applied current and the electroplating solution, is then affected by the presence of these side reactions [47].

Depending on the type of metal used as the anode, it can either be consumed or not during electroplating. The examples of a consumed anode are zinc and copper, and the non-consumable anode are lead and carbon. When a consumable metal is used, it needs to be regularly replaced with a new metal, and for a non-consumable anode, the electrolyte has to be replenished.

2.4.2 Hull Cell

Hull cell is a useful tool to identify the optimal current density to electroplate metal ions for a specific application. Hull cell refers to an electrodeposition tank with a cathode angled with respect to an anode, as shown in **Figure 6**. When the cathode and anode are connected to the external circuit, the circuit becomes complete and current starts to flow.
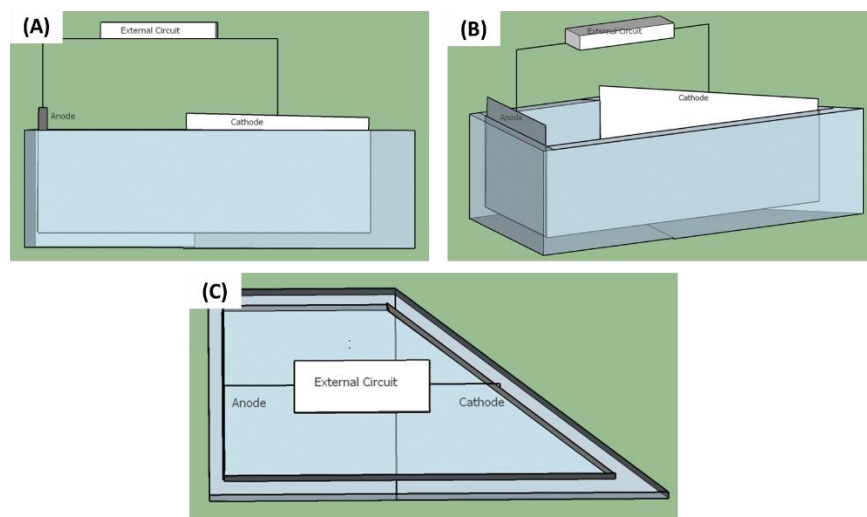
Figure 6 *- Hull cell experimental setup (A) front view of the actual experimental setup showing the external connection (B) side view and (C) top view*

The shape of the Hull cell container is designed such that ions are deposited with varying current densities along the cathode. Hence, the deposits with various current densities can be generated from a single experiment [48]. The results of the Hull cell are shown in **Figure 7**. The left side, placed nearest to the anode, exposed to the highest current density, and the right side the lowest current density. The intensity of the deposits become lighter from left to right – an indication of lower metal deposition.

The local current density at a specific location can be calculated using the following equation [49]:

$$j = I\ (5.10 - 5.24 log_{10}L) \tag{15}$$

Where j is the local current density on cathode (A/dm^2), I is the total current applied to the system (A), and L is the distance from high current density end of panel (cm).

This equation is only valid for the deposits located in between 1 to 8 cm on the cathode and electroplated in 267mL of electroplating solution.

Figure 7 - Zinc deposited on a graphite foil via Hull cell experiment

2.4.3 Parallel Cell

After determining the desired current density from the Hull cell experiment, a parallel cell experiment was performed. Unlike the Hull cell set-up, the cathode and the anode are placed in parallel to each other in the parallel cell. The distance between the two electrodes is obtained from the Hull cell container where the optimal current density was determined. The purpose of conducting the parallel cell experiment was to analyze the deposited sample more accurately.

2.4.4 Treatment of Brass Foil

A brass foil was used as a substrate to deposit zinc ions, and also acted as the current collector in the ReHAB. The brass foil was pre-treated before the electrodeposition of zinc in order to provide a good contact between the substrate and the deposited metal. A good contact between them should result in a small resistance and produce a better battery performance.

T.M.H Saber *et al.* [50] studied various brass treatment methods: degreasing with acetone, mechanical cleaning, acid cleaning, and electrochemical cleaning. They found out that cleaning with acetone did not change the surface of brass, and electrochemical cleaning removed the most of the zinc – changing the alloy concentration, and thus not preferred. For the mechanical cleaning, it removed the oxide layer on the surface of the brass foil, but scratches were present. As for the chemical method, 25 vol. % HNO_3 allowed the dissolution of both copper and zinc, leaving similar composition as the bulk alloy composition. When the authors combined the last two methods, they obtained the optimal results [51].

2.5 Additives

Additives are usually added to an electroplating bath because they take a part in the nucleation and growth process of the deposits. Hence, depending on the choice of additive used during electroplating, the growth behaviour and eventually the properties of the deposit will be affected [52]. Thus, the modified structure of zinc will indeed affect the battery performances.

2.5.1 Fundamentals/Mechanisms of Additives

The behaviour of additives during electroplating can be explained by the mechanisms of chemisorption and physisorption. Chemisorption describes chemical reactions creating covalent bonds between the surface of a substrate and adsorbates. Hence, electron transfer and electron sharing are present. Physisorption, on the other hand, occurs by van der Waals force that attracts adsorbate to the surface of the substrates. This process does not require electron transfer. In most of the cases, additives adsorb and desorb at an equal rate. If the rate is not the same, the additives become a part of the deposits. They also can be consumed in the electrochemical reactions. [48]

How additives affect zinc deposition in real life has been studied by many researchers through experiments. The studies showed that as the additives adsorbed onto a surface, they affect on the kinetics of the electron transfer, the zinc deposition/dissolution, or both [53]. Also, the zinc deposition is hindered due to some of the unavailable active sites taken up by the additives. This process may vary for each additive based on its characteristics and the interaction between the substrate and the additive [54]. The additives also influences the zinc nucleation and its growth orientation by changing the concentration of growth site and anions, diffusion coefficient, and the activation energy of anions [48].

A. Gomes *et al.* [54] found that once the additives (cetyl trimethylammonium bromide (CTAB) and Triton X-100) were adsorbed onto the substrates, the surface available for zinc deposition was blocked and thus, the metal ion deposition was hindered. Moreover, the additives also changed the orientation of the adsorbed layer [48]. The same group (A. Gomes *et al*. [53]) also found out that the orientation of the deposits without additives was (002), and this orientation was changed to (110) and (101) with CTAB and PEG, respectively.

Other than these effects described above, additives can be also used for other purposes, such as leveling and brightening. The purpose of using leveling additives is to even out the roughness on the surface. When uneven current distribution is present, a rough surface is obtained due to the diffusion and the ohmic resistance [48]. This rough surface can be levelled out with levelling agent, which changes the diffusion and ohmic resistance to an active control. By changing into the active control, non-uniform deposition occurs over the rough surface to produce an evenly levelled surface. [48]

The brightening additives, as the name indicates, produces shiny deposits by reducing the size of the crystallites smaller than the visible light wavelength [55]. There are three mechanisms how brightening agents work: diffusion-controlled leveling, grain refining, and random electrodeposition [48].

2.5.2 Categories of Additives

Additives can be categorized into various groups. In this project, they are divided into two categories: organic and inorganic additives. In general, organic additives provide smooth and bright surface by changing the shape and the size of the deposits and increasing the deposition overpotential [53, 54]. As for inorganic additives, they can accelerate metal ion deposition rate [56]. Other than these effects, some of the organic and inorganic additives increase the corrosion resistance [57]. Each additive influences the deposition in its unique way, and combination of two or more additives may generate synergistic effects.

Shanmugasigamani *et al.* [58] studied the effects of the organic additive, polyvinyl alcohol (PVA), during electroplating zinc in a cyanide-free alkaline bath. The Hull cell set-up was used to deposit zinc in the non-cyanide bath containing zinc oxide and sodium hydroxide. When PVA was added into the alkaline electroplating baths, the current efficiency at the cathode was improved and refined grain deposit was obtained. Also, the speed of the rate-determining step was controlled by PVA because it was able to entrap zinc hydroxyl anions.

J.C. Ballesteros *et al.* [59] studied the effect of polyethylene glycol 20000 (PEG) on zinc electrodeposition process in a chloride bath. The authors found out that PEG first was adsorbed onto a substrate and then desorbed back into the electrolyte. With the presence of PEG, 0.71mg of zinc was deposited in the potential range of -0.4 to -1.7V, whereas only 0.66mg was deposited without PEG [59]. Thus, PEG was able to increase the zinc deposition rate.

 C. Hu *et al.* [37] selected three additives – tetra-ethylene-pentamine (TEPA), potassium diphosphate (PDP), and potassium sodium tartrate tetraphydrate (PSTT) – to electroplate zinc in a sulfate bath. The smoothest surface was obtained when PDP was used, and followed by PSTT. Between the two, higher stripping efficiency was achieved with PSTT (62.4%) than that with PDP (40.6%) [37]. When TEPA was used, dendrites were formed rather than a smooth surface – hence, it was not favoured.

2.6 Physical Characterization Techniques

2.6.1 X-ray Diffraction (XRD)

X-ray diffraction (XRD) is an experimental tool used for studying the crystal structures of materials. XRD determines the crystallinity of a material based on the constructive interference created as incident rays interact with the sample. More specifically, photons from the radiation interact with the electrons in an atom, creating unique waves as shown in **Figure 8**. The obtained data provides the information about the crystal structures of the materials.
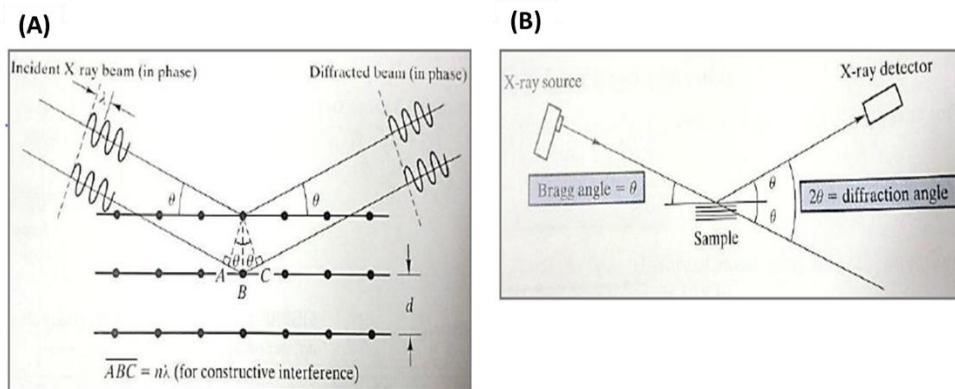
Figure 8 - (A) Schematic of x-radiation for a simple crystal lattice
(B) Relationship between the Bragg angle and experimentally measured diffraction angle[60]

The relationship between the wavelength of the rays and the material can be expressed with Bragg's law:

$$n\lambda = 2dsin\theta$$

Where n is the order of diffraction, d is the spacing between two adjacent planes of atoms, λ is the wavelength of the electromagnetic radiation, and θ is the scattering angle (or Bragg's angle).

In order to identify the coordinate of the planes or distance between the planes, following equation is used:

$$d_{hkl} = \frac{a}{\sqrt{h^2 + k^2 + l^2}}$$

Where a is the lattice parameter; and h, k, and l are the Miller indices plane coordinate in x, y, and z-direction.

2.6.2 Scanning Electron Microscopy (SEM)

Scanning electron microscopy (SEM) is a tool used to understand the topology of materials in micro and nano scale. How SEM works is that as it sends out a beam of high energy electrons to a sample, signals are produced during the electron-sample interaction. The signals, collected by the electron collector, contain the information about the sample, such as morphology and chemical composition of the materials. This technique is carried out in a vacuum chamber to minimize the interference during the interaction between the sample and the electrons. If the material is not conductive, it may be charged during the process, which creates difficulties in image acquisition. Thus, non-conductive materials may be coated before the collection of images.

2.7 Electrochemical Characterization Techniques

2.7.1 Float Current

Float current is a current required to compensate for the capacity lost during the self-discharge of a battery. After the battery is fully charged and is at stationary state, the unwanted side reactions occur, causing the battery voltage to decrease. To keep the battery at full capacity, current is constantly applied to the battery. Measuring the amount of current (or float current) needed indirectly indicates the amount of side reactions occurring in the battery after fully charged. For the industry applications, smaller float current is desired.

2.7.2 Corrosion Test

Corrosion behaviour of zinc metal is studied with Tafel extrapolation and the polarization resistance methods. Tafel extrapolation method is used to determine the corrosion rate of a metal in an aqueous solution by applying mixed potential theory [27]. When corrosion occurs on a metal, a cathodic and an anodic reactions occur. The combination of these half-cell potentials from these reactions (or polarization of two potentials to the same intermediate potential) is called corrosion potential, E_{corr}, or mixed potential.

This method is carried out with linear polarization technique, which scans an electrode over a range of voltages and measures the resulting current. With the obtained data, a semi-log plot is

generated, shown in **Figure 9**. The corrosion rate of a metal can be determined from the slope of the linear region [27]. By extrapolating linear regions on the cathodic and anodic curves, corrosion potential, E_{corr}, and corrosion current density, i_{corr}, are determined. The value of cathodic corrosion current density (i_c) is the same as the value of anodic current density (i_a).
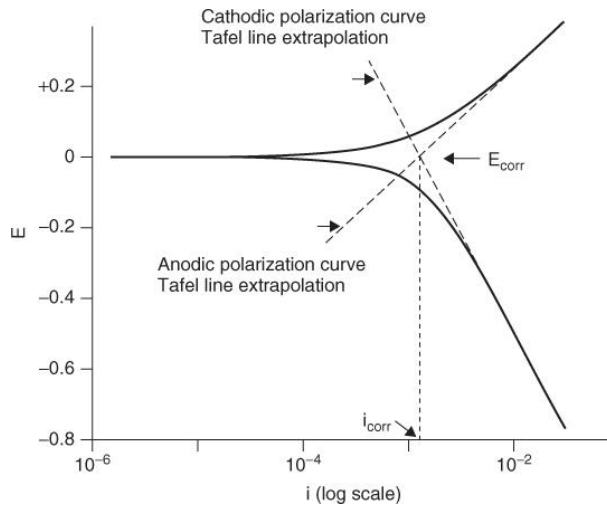
Figure 9 - Tafel curve with line extrapolation indicating corrosion parameters [61]

Determined corrosion current can provide information about corrosion rate because the corrosion current is proportional to the corrosion rate. Their relationship is expressed as follows:

$$\text{Corrosion rate} = \frac{0.13 I_{corr}(E.W)}{d}$$

Where E.W. is the equivalent weight of the sample, and d is the sample density.

Another method to understand the corrosion of a metal is the polarization resistance, Rp. By assuming a small overpotential, the polarization resistance (Rp) can be calculated using:

$$R_p = \frac{B}{i_{corr}} = \frac{\frac{\beta_a \beta_c}{2.3 (\beta_a + \beta_c)}}{i_{corr}}$$

Where β_a and β_c are the anodic and cathodic Tafel constants, which can be determined with

$$\epsilon_a = \beta_a \log \frac{i_a}{i_{corr}}$$

23

$$\epsilon_c = \beta_c \log \frac{i_c}{i_{corr}}$$

Where ϵ_a and ϵ_c are the anodic and cathodic polarization/overvoltage, i_{corr} is the corrosion current density, and i_a and i_c are anodic and cathodic current density.

The overvoltage can be expressed as:

$$\epsilon_{c/a} = E_{c/a} - E_{corr}$$

Where E_{corr} is the mixed potential, and $E_{c/a}$ is applied potential.

By combining the two overpotential equations, Tafel constants can be determined. If there are unknown corrosion parameters, then the slopes of the cathodic and anodic linear regions in the Tafel plot can be used as β_a and β_c, respectively. These values are then used to calculate Rp. If the metal has high Rp, it is highly resistance to corrosion.

2.7.2 Galvanostatic Charge-Discharge

ReHABs with the synthesized anodes and the commercialized zinc foil are galvanostatically cycled between 1.4 to 2.1V. Typical galvanostatic charge and discharge profiles are shown in **Figure 10a**.
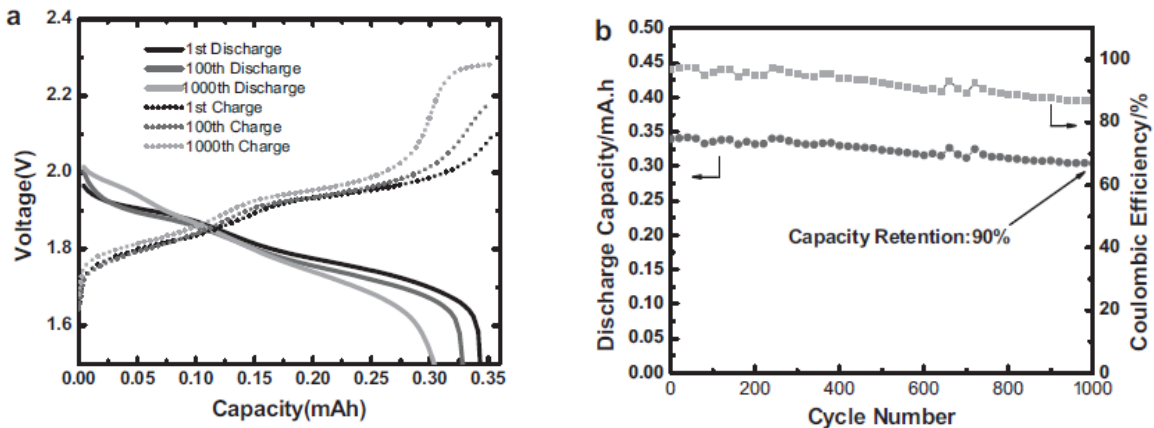
Figure 10 - *(a) A typical galvanostatic charge and discharge profile of ReHAB operated at 4C*
(b) cyclability and coulombic efficiency of ReHAB with undoped LiMn₂O₄ [3]

Both charge and discharge curves show two different plateaus, an indication of two-phase lithium extraction and intercalation processes [3]. As the number of battery cycle increases, the

24

polarization of the battery also increases. This leads to the discharge capacity and coulombic efficiency to decrease as shown in **Figure 10b**. After the cyclaiblity test, the capacity retention can be calculated with the capacities from the first and the last cycle.

Chapter 3. Synthesis of Zinc via Electroplating with Additives

3.1 Introduction

Since the invention of rechargeable aqueous batteries, the studies of new materials for the electrodes have been carried out. In this project, ReHAB was selected. ReHAB consists of lithium manganese oxide ($LiMn_2O_4$) as the cathode active material. $LiMn_2O_4$ is a good candidate as a cathode material in the aqueous batteries because tightly bounded lithium ions make $LiMn_2O_4$ stable in air and water [6]. Also, it shows a small volume variation between lithiated and non-lithiated states [3]. As for the anode, zinc metal was selected because of its low redox potential, good reversibility, high over-potential for hydrogen evolution in acidic environment, large specific capacity, good corrosion resistance, and cost effectiveness [3, 14, 15].

Theoretically, an ideal performance is expected from ReHAB, but in reality, there are still some rooms to improve. This project was focused on the modifications of the zinc anode. When zinc is utilized in the aqueous batteries, a few problems associated with zinc metal arises. They are:, metal corrosion, dendrite formation, and hydrogen gas (H_2) evolution [5, 16]. In order to alleviate these problems, many studies [17, 18, 21-23] have been conducted to mitigate the aforementioned problems with zinc metal.

In this project, zinc was synthesized via electroplating with additives. 7 additives (4 organic and 3 inorganic additives) were selected to modify the structure of the zinc deposits. The performance of the zinc with these additives were then analyzed via XRD, SEM, battery and corrosion tests.

3.2 Experimental Procedures

3.2.1 Battery Components

3.2.1 Cathode

The synthesis of the cathode was carried out as described: 86 wt.% analytical grade of $LiMn_2O_4$ (MTI Co.), 7 wt.% KS-6 graphite (Timcal), and 7 wt.% polyvinylidene fluoride (PVDF, Kynar, HSV900) were mixed in n-methyl-2-pyrrolidone (NMP, Sigma-Aldrich Co., 99.5% purity) using Planetary Centrifugal Mixer (AR-100, ThinkUSA) for 2 minutes. The mixed slurry was then casted on a graphite foil (Alfa Aesar, 99.8%) and placed in 60°C vacuum chamber for 3 hours. The dried slurry was cut in a circle with 12mm diameter.

3.2.2 Electrolyte

A mixture of zinc sulfate and lithium sulfate was used as the electrolyte. 1M zinc sulfate heptahydrate (Alfa Aesar Co., 98%) and 2M lithium sulfate (Sigma, 98%) were dissolved in DI water, and its pH was adjusted to 4 using sulfuric acid.

3.2.3 Separator

The separator used in the batteries was absorptive glass mat (AGM, NSG Corporation). It is highly porous that it can absorb a large amount of electrolyte.

3.2.2 Anode Preparation

3.2.2.1 Electroplating Solution

The electroplating solution was prepared by dissolving 0.6M zinc sulfate (Alfa Aesar, 98%), 0.1M ammonium sulfate (Sigma, 99%), and 100ppm of additive in Di-water. The selected additives were: cetyl trimethylammonium bromide (CTAB, Signma, 98%), sodium dodecyle sulfate (SDS, Signma, 99%), polyethylene glycol 8000 (PEG, Signma, MW 8000, 99%), thiourea (Alfa Aesar,

99%), indium (II) sulfate (Sigma, 99.99%), tin (IV) oxide (Sigma, 99.9%), and boric acid (Signma, 99.5%). Each of the additives was added to the electroplating bath individually.

3.2.2.2 Hull Cell

Hull cell experiment was carried out in a plastic Hull cell container as shown in **Figure 6**. The consumable anode, in this case zinc foil, was placed on the left side of the container, and a cathode on the right. As according to the theory, 267mL of the electroplating solution was used in each experiment. Direct current (1A and 1.5A) was applied using BK Precision machine to the Hull cell set-up for 10 minutes at room temperature. Then, the synthesized samples were dried overnight in air.

3.2.2.3 Parallel Cell

The parallel cell set-up is shown in **Figure 11**. A cathode and an anode were placed 5cm apart facing each other. For the parallel cell experiment, 100mL of electroplating solution was used. The electrodes used in the parallel cell were the same as those used in the Hull cell. Direct current was introduced to the system using BK Precision for 10 minutes. After the synthesis, the samples were dried overnight in air.
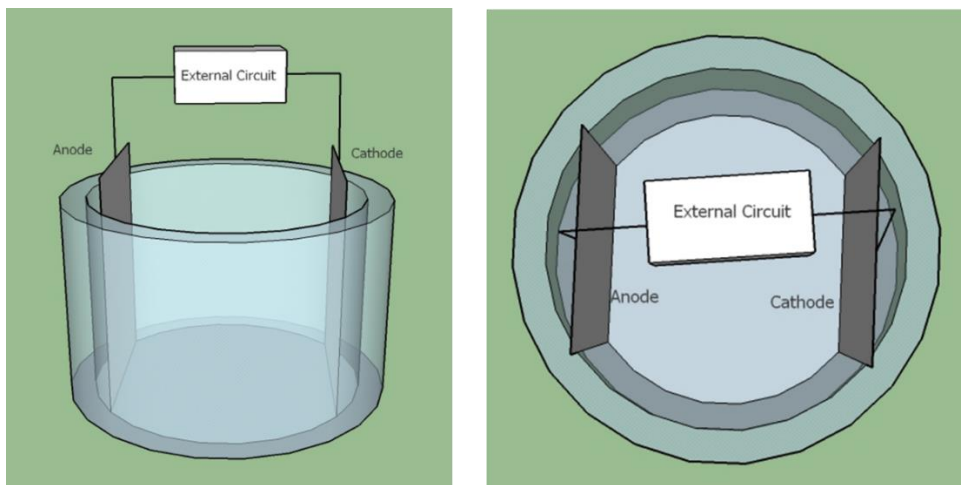
Figure 11 - Schematics of parallel cell (a) front and (b) top view

3.2.2.4 Substrates

Two different substrates were selected: graphite (Alfa Aesar, 99.8%) and brass foil. The graphite foil was selected because a good battery performance was observed when it was used as the substrate for the cathode in ReHAB. The brass foil was chosen as another type of substrates to deposit zinc on. A good contact between the zinc deposits and the brass foil was assumed to be made as brass contains zinc. This hypothesis was verified through experiments.

There was no treatment done on the graphite foil. As for the brass foil, the optimal brass treatment was determined by comparing different treatment methods.

3.2.2.4.1 Brass Foil Treatment

In this project, four treatment methods were selected: no treatment, mechanical, chemical, and the combination of mechanical and chemical methods. As for the mechanical treatment, the surface of the brass foil was sanded using a sand paper. After the sanding, the brass was washed with DI water to remove any residuals left on the surface.

As for the chemical treatment, it was carried out using nitric acid (HNO_3). After the brass foil was cut into an appropriate size, it was dipped into 25 vol. % HNO_3 solution for 5 seconds, and thoroughly washed with DI water. Then, it was dried in air.

After each treatment, the brass foil was used as the substrate to deposit zinc.

3.2.3 Characterization Technique Conditions

The crystallinity of the synthesized anode was analyzed with D8 Discover power x-ray diffraction (XRD, Bruker Co., CuK$\propto$ 1.5406Å , 40kV, and 40A). The samples were scanned (*ex*-situ) over 2 theta range 10 to 90° at the rate of 0.003 °min^{-1} with LynxEye detector. The XRD results were analyzed with the Bruker XRD search match program EVATH.

The morphologies of the synthesized anodes were examined with field emission scanning electron microscopy (FE-SEM, Carl Zeiss Ultra Plus Field Emission SME, Zeiss Co.), operated at 10kV.

The corrosion data of the as-prepared samples and the commercialized zinc was collected with VMP3 potentiostat/galvanostat (Bio-Logic Science Instrument Co.). The corrosion current and potential were measured in a three electrode cell system by applying linear polarization technique. The working, counter, and reference electrodes were zinc, platinum, and Hg/Hg_2SO_4, respectively. The electrode was scanned between -0.25V to 0.25V from its open circuit voltage (OCV) at the rate of 0.166mV/s. The surface area of the tested electrode was ~1cm^2. It was used to convert corrosion current density (i_{corr}) to corrosion current (I_{corr}).

The cycle life of the batteries with the synthesized and the commercialized anodes were tested in coin cell type batteries. These batteries contained the cathode, electrolyte, anode, and the separator as described in the above sections. The galvanostatic charge-discharge cycling of the batteries were carried out at room temperature at 4C rate (1C = 120mAh/g) with NEWWARE battery tester [14] (NEWWARE Battery Test System, Neware Co. Ltd., China). The battery was cycled between 1.4V to 2.1V.

The same battery tester was used to perform the float current test. For this test, two-electrode SwagelockTH-type cells were used. The potential of the batteries were maintained at 2.1V for 7 days at room temperature, and the current necessary to maintain the potential was recorded.

3.3 Result and Discussion

3.3.1 Determining Zinc Electroplating Condition

Before the synthesis of zinc with the additives, the electroplating conditions to deposit the minimum amount of zinc required to run ReHAB as the one with commercialized zinc foil (Rotometals, thickness 0.2mm) were determined. Since there were two unknown variables – the current density and the deposition time, two experiments were carried out. In the first experiment, deposition time was fixed to find the optimal current density to synthesize zinc that can produce good ReHAB performance as the one with the commercialized zinc; and in the second experiment, the deposition time was varied by fixing the determined current density in the previous experiment to investigate how deposition time affects the performance of ReHAB.

These experiments were done in the Hull cell set-up. Just to note that zinc deposition in this section was carried out on the graphite foil substrate.

As shown in **Table 1**, the deposition time was fixed to 10 minutes for all the samples, and they were deposited with different current densities (30, 50, and 80 mA/cm^2). This experiment also indicated what morphology of zinc would be suitable in ReHAB system because morphology of a deposit changes with current density.

Table 1 - Summary of deposited samples with zinc deposition time and corresponding current densities

Sample #	Deposition Time (min)	Current Density (mA/cm^2)
1		30
2	10 min	50
3		80

After the electrodeposition of zinc, the samples were tested in ReHAB, and their results are shown in **Figure 12**. The battery with the zinc electroplated with 30mA/cm^2 showed fast capacity fading in comparison to the ones with higher current densities and the commercialized zinc foil. The batteries with 50 and 80 mA/cm^2 showed comparable battery performance as the ones with the commercialized zinc foil. Hence, it was enough to use 50mA/cm^2 to electroplate zinc as the battery with this anode could maintain high capacity as the commercialized zinc foil battery.

Figure 12 *- Cyclaiblity of ReHAB with synthesized zinc anodes electroplated at current densities
of 30, 50, 80 mA/cm² for 10min and commercial zinc foil (Commercial)*

The next experiment was to investigate how the performance of ReHAB would change with deposition time. For this experiment, the current density was fixed at 50 mA/cm² and the deposition time was varied from 6 to 20 minutes.

Table 2 *- Summary of the deposited samples with their zinc deposition time and corresponding current densities*

Deposition Time (min)	Current Density (mA/cm2)
6	
8	
10	50
15	
20	

Figure 13 is the cyclability of ReHAB with the zinc anodes electroplated for various deposition time. When ReHAB employed the anodes electroplated for 6 and 8 minutes, the capacities of the batteries were lower than the one with zinc electroplated for 10 min. When the zinc deposition time was higher than 10 min, very similar battery performance was observed as the one

electroplated for 10 min. Hence, the current density of 50mA/cm^2 and the deposition time of 10 min were selected as the electroplating conditions to synthesize zinc anodes.

Figure 13 *- Cyclaiblity of ReHAB with synthesized zinc anodes electroplated at 50mA/cm^2 for deposition time of 6, 8, 10, 15, 20min and commercialized zinc foil (Commercial)*

3.3.2 Treatment of Brass Foil

Before using the brass foil as a substrate for the anode, the surface of the brass underwent three different treatments. Firstly, two treatment methods were compared: mechanical and chemical treatments. After the treatment, zinc ions were deposited on the treated surface of the brass foil. The performance of ReHAB with these anodes is shown in **Figure 14**.
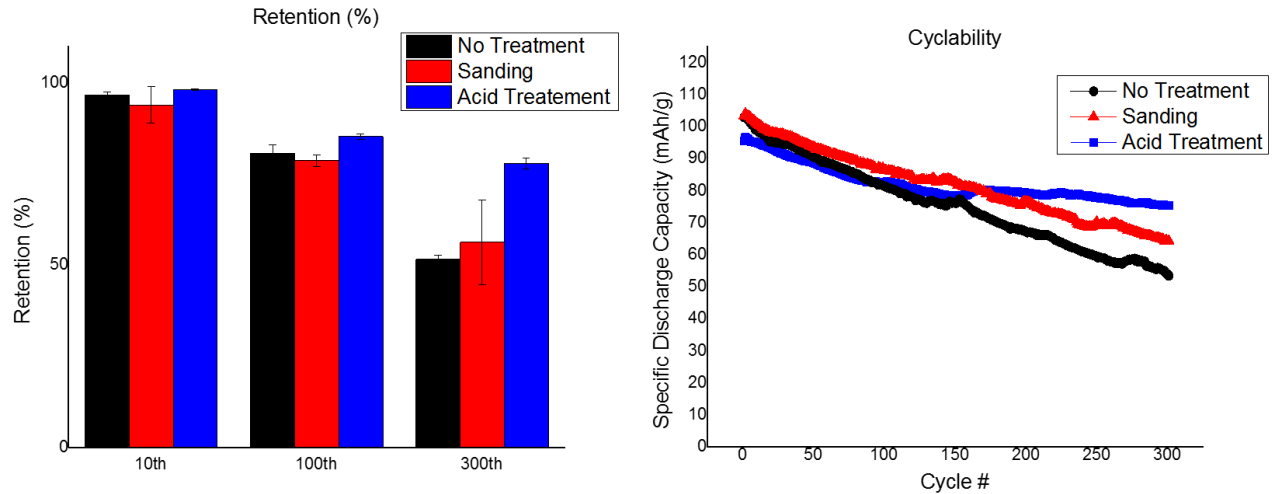
Figure 14 - Result of the discharge capacity retention and the cyclability plot from ReHAB with brass foil substrate exposed to different treatments (Hull cell result)

When there was no treatment done on the brass foil, the lowest discharge capacity retention of 50% was obtained at the 300th battery cycle. The highest capacity retention was found when the brass foil was treated with nitric acid.

The capacity was well maintained when the brass foil was treated with nitric acid. This implies that a good contact between the substrate and the electroplated zinc was achieved when the surface was treated with acid. The mechanical sanding showed better battery performance than the one without any treatments, but its performance was worse than the one with chemically treated brass foil substrate. At the 300th cycle, the average capacity retention of ReHAB with the mechanical sanding was smaller than that with the acid-treated brass foil. Also, a large error bar indicated polishing with the sandpaper is unreliable. Therefore, the treatment with nitric acid was preferred and selected.

In the next experiment, the effect of combining the mechanical and chemical methods was investigated as T.M.H Saber *et al.*[50] achieved the optimal results (oxide-free and scratch-free brass surface) by combining the two methods. The performance of ReHAB with this substrate is summarized in **Figure 15**.
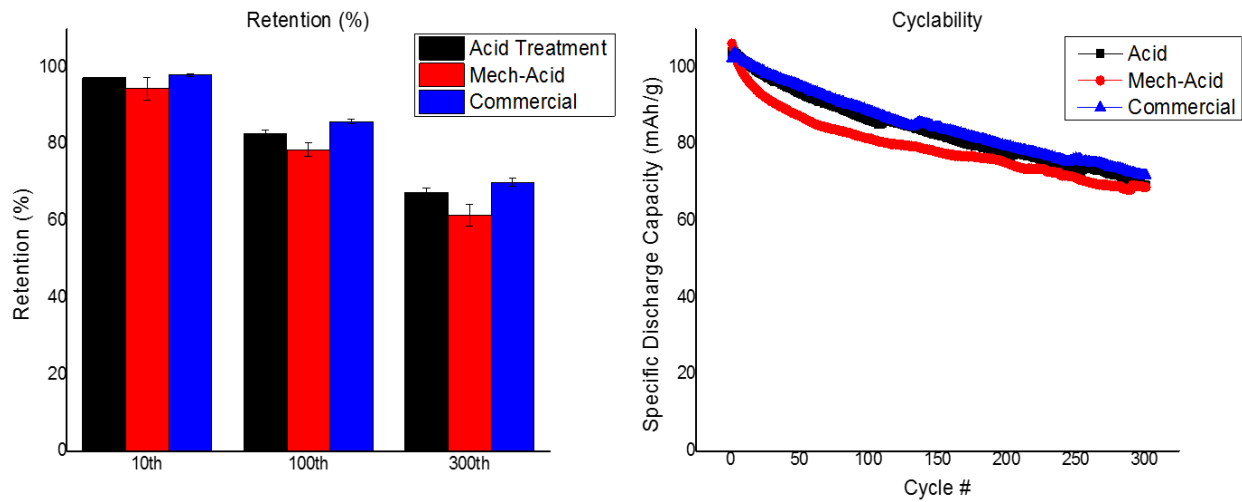
Figure 15 *- Result of the discharge capacity retention and the cyclability plots from ReHAB with brass foil substrate exposed to different treatments (Parallel cell result)*

The effect of combining the mechanical and chemical treatments, which is labelled as 'Mech-acid,' is shown in **Figure 15**. As shown in the capacity retention and cyclability plots, the performance of ReHAB with the brass treated with both methods generated similar performance as the one with the brass foil treated with only acid. Hence, modifying the surface of the brass foil with only acid was sufficient to produce good ReHAB performance. Therefore, only nitric acid was used to treat the brass foil to enhance the contact (or reduce the resistance) between the brass foil and the deposits.

3.3.3 Comparison of Two Substrates – Graphite and Brass Foils

The comparison of two substrates (graphite and brass foil) was carried out in this section. In the beginning of the project, the graphite foil was primarily used, but its flexible property led the graphite foil to be easily torn. Thus, the brass foil was chosen to replace the graphite foil as the substrate for zinc ion deposition.

In order to identify whether the performance of ReHAB with the brass foil was compatible as that with the graphite foil, ReHAB was assembled with these substrates. The performance of ReHAB with the zinc anode electroplated on the graphite and the acid-treated brass foil is shown in **Figure**

16. ReHAB with brass foil is labelled as 'Acid Treated,' and the battery with graphite foil as 'Graphite Foil.'
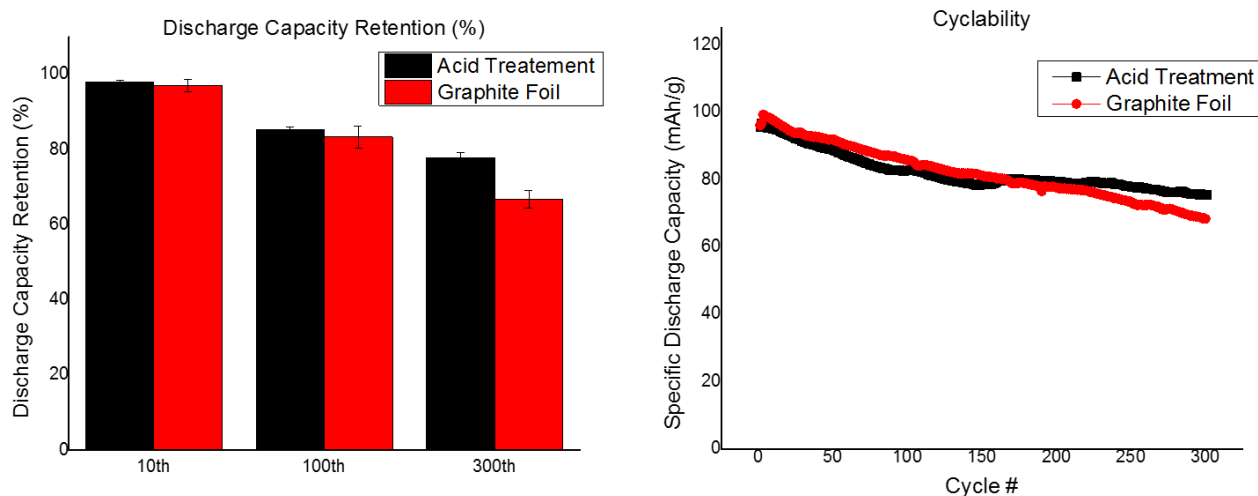
Figure 16 *- Result of the discharge capacity retention and the cyclability plots from ReHAB with graphite and brass foil as anode substrates (Hull cell result)*

From the results shown above, about 17% higher capacity retention was observed with ReHAB with the acid treated brass foil than that with the graphite substrate at the end of 300th cycle. In other words, the battery capacity was well maintained when brass foil was used as the substrate for the anode. Thus, only brass foil was used as the substrate (in electroplating) and the current collector (in ReHAB).

3.3.4 Optimal Additive Concentrations

The amount of additive used during electroplating influences the property of the deposits, and thus, many studies [62-66] have been carried out to determine the optimal additive concentrations. In this section, the optimal additive concentrations were identified.

In order to compare the effect of each additive fairly, the optimal concentration of each additive was required. In this project, however, one of the additives was randomly selected and its optimal concentration was assumed to be equal to the optimal concentration of the rest of the additives due

to the time constraint. The randomly selected additive was boric acid, and its optimal concentration was determined in this section.

For identifying its optimal concentration, four different concentrations of boric acid were selected: 0, 50, 100, and 500ppm.
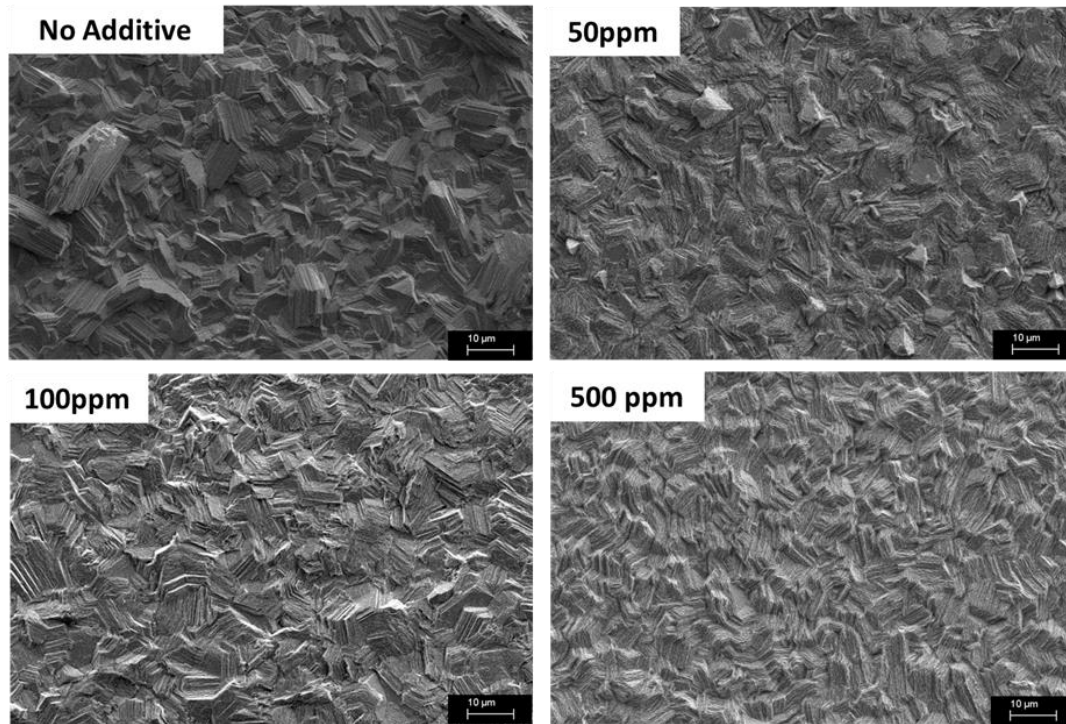
Figure 17 - *SEM images of zinc deposits with 0 (no additive), 50, 100, and 500ppm of boric acid in electroplating bath (magnification 1k)*

With different concentrations of boric acid, different morphologies were obtained. The SEM images indicated that in general, stacks of irregular platelets were generated as shown in **Figure 17**. Similar structure to these SEM images was also seen in C. Hu *et al.* [37]. This kind of structure is obtained when high current density is applied to deposit zinc ions [67]. With smaller current density, the morphology of the zinc deposits created in a zinc sulfate solution would become regular hexagonal crystalline structure [53, 67].

When there was no additive used, the zinc deposits were coarse and irregular. As the concentration of boric acid increased, the size of the deposits became smaller and more uniform. From the SEM images, 100 and 500ppm of boric acid produced uniformly distributed zinc deposits.
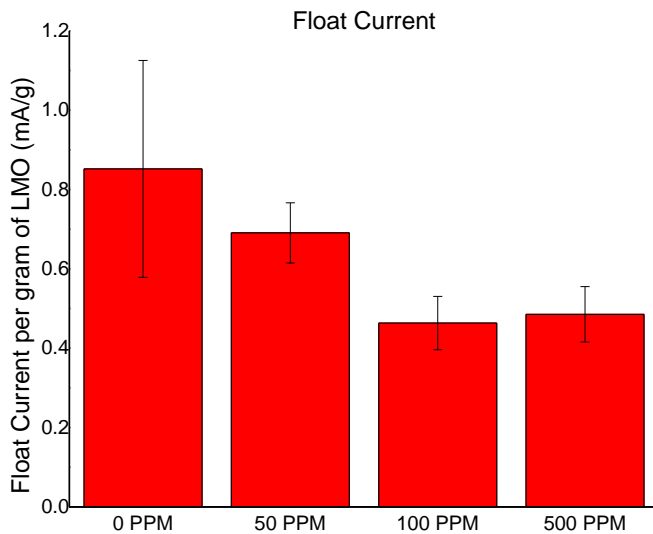
Figure 18 *- Float current of ReHAB with electroplated anode with 0, 50, 100, and 500ppm of boric acid in electroplating bath*

The float current results are plotted in **Figure 18**. The battery with the anode electroplated without the additive (labelled as '0 ppm') presented the highest float current. When higher concentration of boric acid was employed to synthesize the zinc deposits, smaller float current was obtained. In other words, the zinc electroplated with higher concentrations of boric acid reduced the side reactions occurring in the batteries when they are not in use. When the concentration of boric acid exceeded 100ppm, however, the amount of float current remained about the same.

Table 3 *- Summary of corrosion potential and current of the electroplated anode*
with 0, 50, 100, and 500ppm of boric acid in electroplating bath

	Corrosion Potential (mV)	**Corrosion Current (uA)**
0 PPM	-1429 ± 5	1136 ± 82
50 PPM	-1428 ± 7	133 ± 14
100 PPM	-1419 ± 9	156 ± 13
500 PPM	-1422 ± 8	160 ± 23

Table 3 presents the corrosion potentials and currents of the synthesized zinc obtained by analyzing their Tafel plots. From the results, the zinc deposited without additives showed the highest corrosion current. This may be due to the modified crystalline structure using boric acid

during the zinc deposition as shown in **Figure 19**. When there was no additive used during electroplating zinc, the strong peak of (103) was shown. With the presence of boric acid (100ppm), the crystalline orientation was favoured in (002). Hence, the corrosion rate may be increased if a sample consists of a strong peak of (103).
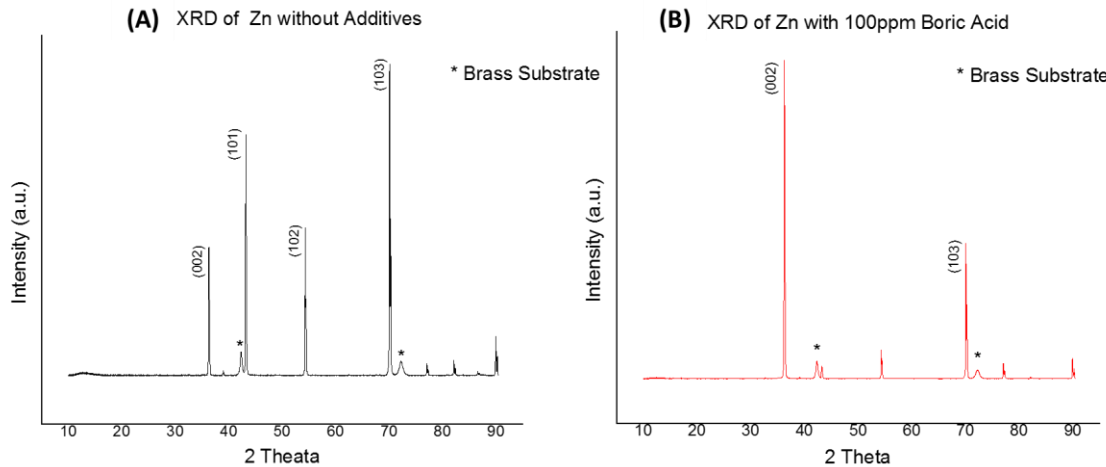
Figure 19 - *XRD of zinc electroplated (A) without additives and (B) with 100ppm of boric acid*

The values of the corrosion currents were similar between the zinc electroplated with any concentrations of boric acid, but the values slightly increased with the concentration of boric acid. In other words, overuse of boric acid was not preferred.

Based on these results, 100 ppm of boric acid was determined to be the optimal concentrations as the zinc produced with this concentration not only showed the uniform deposits, but also reduced the float current and corrosion rate. The anode produced with 500 ppm of boric acid also generated similar results as that with 100 ppm. Hence, there was no need to use higher concentration of boric acid as smaller dose produced about the same results. Therefore, 100 ppm was chosen as the optimal concentration for boric acid, and it was assumed to be the optimal concentrations for the other additives as well.

3.3.5 Effect of Organic Additives

In this project, four organic additives were selected: cetyl trimethylammonium bromide (CTAB), sodium dodecyle sulfate (SDS), polyethylene glycol 8000 (PEG), and thiourea.

Many literatures investigated the effect of the selected additives on the synthesis of zinc via electroplating:

1. CTAB: reduction in grain size [53], corrosion inhibitor [68]
2. SDS: corrosion inhibitor [69], hydrogen evolution inhibitor during electroplating [54]
3. PEG: hydrogen adsorption inhibitor, enhancement of current efficiency during electroplating [70], corrosion inhibitor [71]
4. Thiourea: hydrogen evolution inhibitor during electroplating [70], corrosion inhibitor [72]

In order to analyze the effect of the zinc electroplated with these additives, the studies on the zinc electroplated in additive-free solution (Zn-No) and the commercialized zinc foil were also conducted.

3.3.5.1 XRD Result

The XRD results of the synthesized zinc with the organic additives and the commercialized zinc are shown in **Figure 20** and **Figure 22**. The XRD of the zinc electroplated without additives is presented in **Figure 21** to show how additives modified the crystalline structure of zinc.

According to the XRD of the synthesized and the commercialized zinc, the zinc crystals were growing in various orientations. As for the commercialized zinc foil, the highest intensity peak was found at 42°, indicating zinc growth mostly in (101) orientation. The other significant planes were (102), (103), (100), (002), (110), (112), (200), and (201). These peaks were also seen in literature [53, 68].

The morphology of the commercialized zinc is shown in **Figure 20**. Flat and smooth surface with defects (holes) were observed. These holes may be produced during its synthesis. The performance of the commercial zinc will be discussed in the later part of the thesis.

XRD of Commercialized Zinc Foil
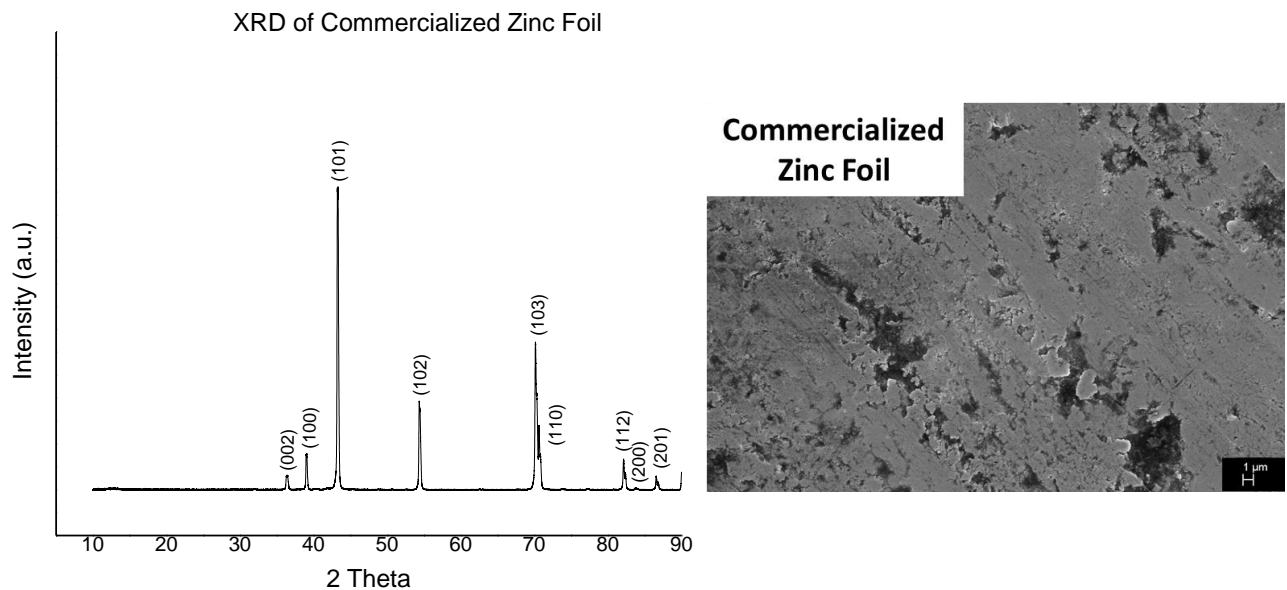
Figure 20 - *XRD and SEM images of the commerciali zinc foil*

XRD of Electroplated Zinc without Additive
(Lower Current Density)

XRD of Electroplated Zinc without Additives
(High Current Density)
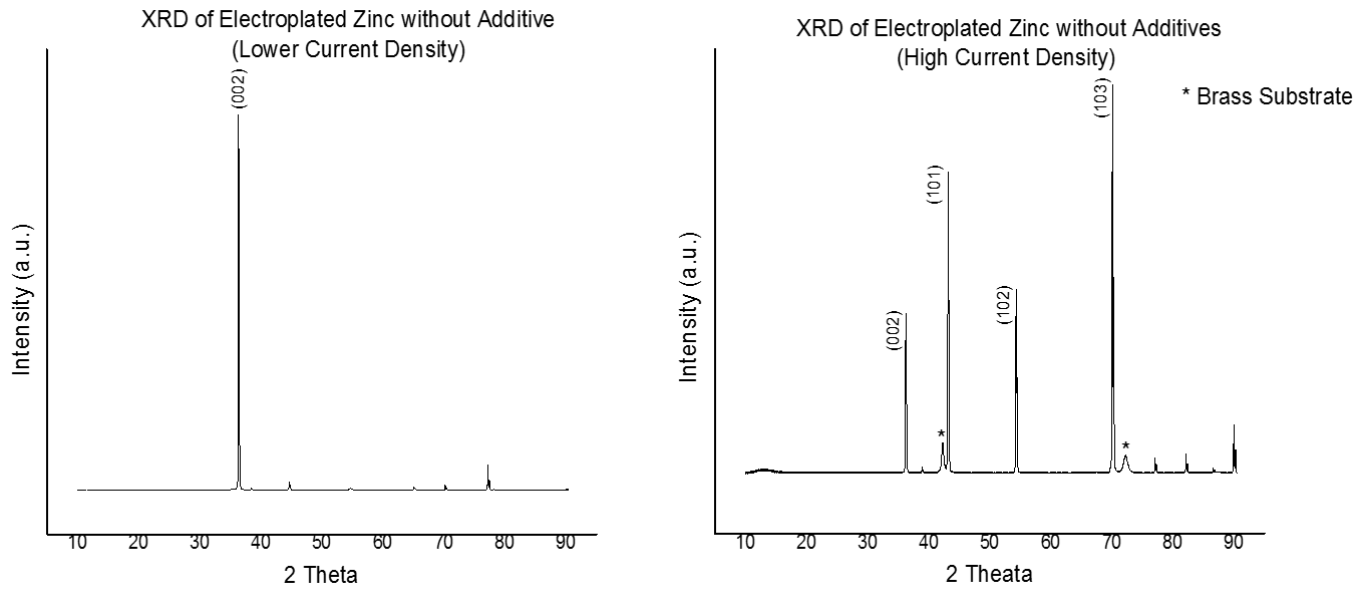
Figure 21 - *XRD of the electroplated zinc without any additives at low and high current densities.*
For lower current density XRD was obtained from Hull cell, and the high current density from parallel cell
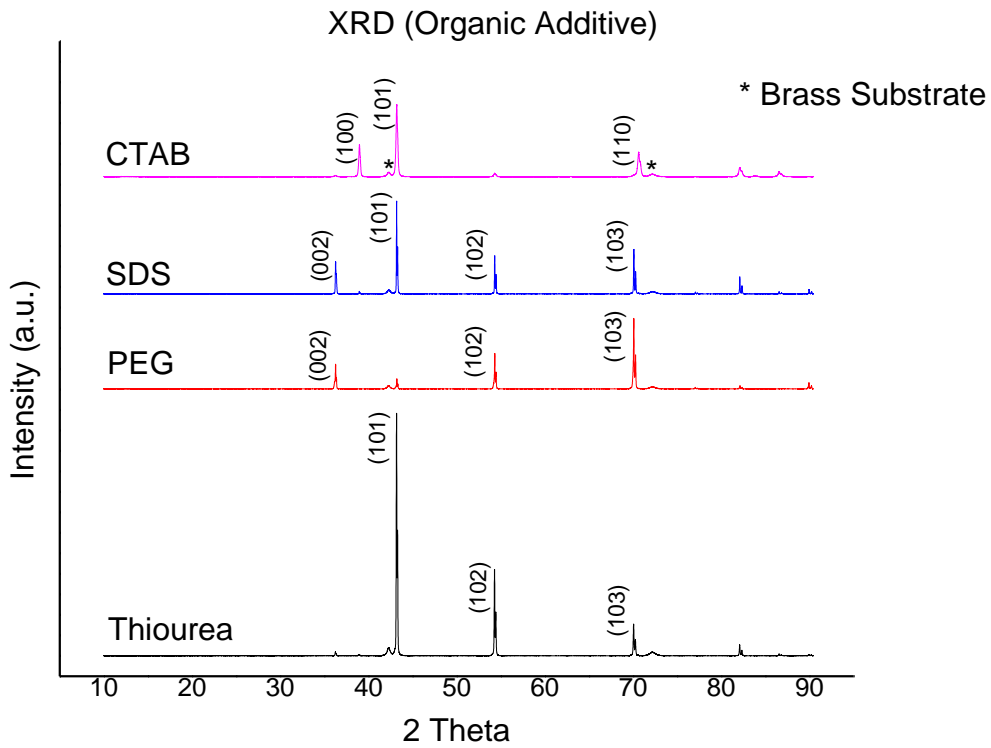
Figure 22 - XRD results of the zinc anode electroplated with organic additives

When no additive was used during the zinc deposition with low current density, the preferred orientation was (002), which was consistent with literature [53, 68]. With higher current density (experiment done in the parallel cell), the growth orientation was mostly directed in (103). This indicates that current density plays an essential role in metal plating. Between the two samples, the one electroplated with higher current density was used to compare with the zinc electroplated with the organic additives.

The XRD of the electroplated zinc with the organic additives, shown in **Figure 22**, consisted of the same zinc peak locations as the commercialized zinc foil and literature [53, 65]. The intensities of the peaks, however, were not the same, indicating different crystalline growth. It is clear that each of the organic additives produced a unique crystalline structure as the peak intensities were different. The changes in the crystallinity of the sample suggests that during electroplating, the additives altered the surface energy because crystals tend to grow in the direction with the lowest surface energy [53]. Not only that, but also the experimental procedure may be another factor contributing to the variations in XRD peak intensity [53].

The usage of CTAB, SDS and thiourea during the zinc deposition (Zn-CTAB, Zn-SDS, Zn-TU) led a strong orientation at (101), which was also seen in literature [62, 64, 73]. The dominant (101) peak was also found in the XRD of the commercialized zinc foil. The changes in the preferential growth from (103) to (101) suggests that CTAB, SDS, and thiourea modified the electroplated anode to become more like the commercialized zinc foil. Also, Machinnon *et al.* [74] explained that having the preferential growth of zinc in (101) implies that high current efficiency was achieved when zinc ions were deposited. This finding is in accordance with D.J. Mackinnon *et al.* [75]'s data of high zinc deposition efficiency obtained with organic additives.

As for the zinc electroplated with PEG (Zn-PEG), zinc crystalline was mostly oriented in (103). Although the preferential orientation of Zn-PEG was the same as that of Zn-No, PEG significantly reduced the peak representative in (101) planes, which was the second dominant peak of Zn-No. According to D.J. Mackinnon *et al*. [74], the preferred orientation of (103) represents that zinc was deposited with low current efficiency. K. Song *et al*. [70] also found that the addition of polyethylene glycol (MW = 2000) reduced zinc deposition efficiency.

Zn-CTAB showed the second highest peak intensity in (100), whereas the commercialized zinc showed in (103). As for Zn-SDS anode, SDS relatively enhanced the growth of (002) and (102) planes, and inhibited (100) plane. The XRD of Zn-TU indicated that some of planes were oriented in (102) and (103), but their intensities were much lower than (101) – in other words, thiourea enhanced the zinc growth only in one orientation. As for Zn-PEG, it also showed zinc plane orientation in (002) and (102).

3.3.5.2 SEM Result
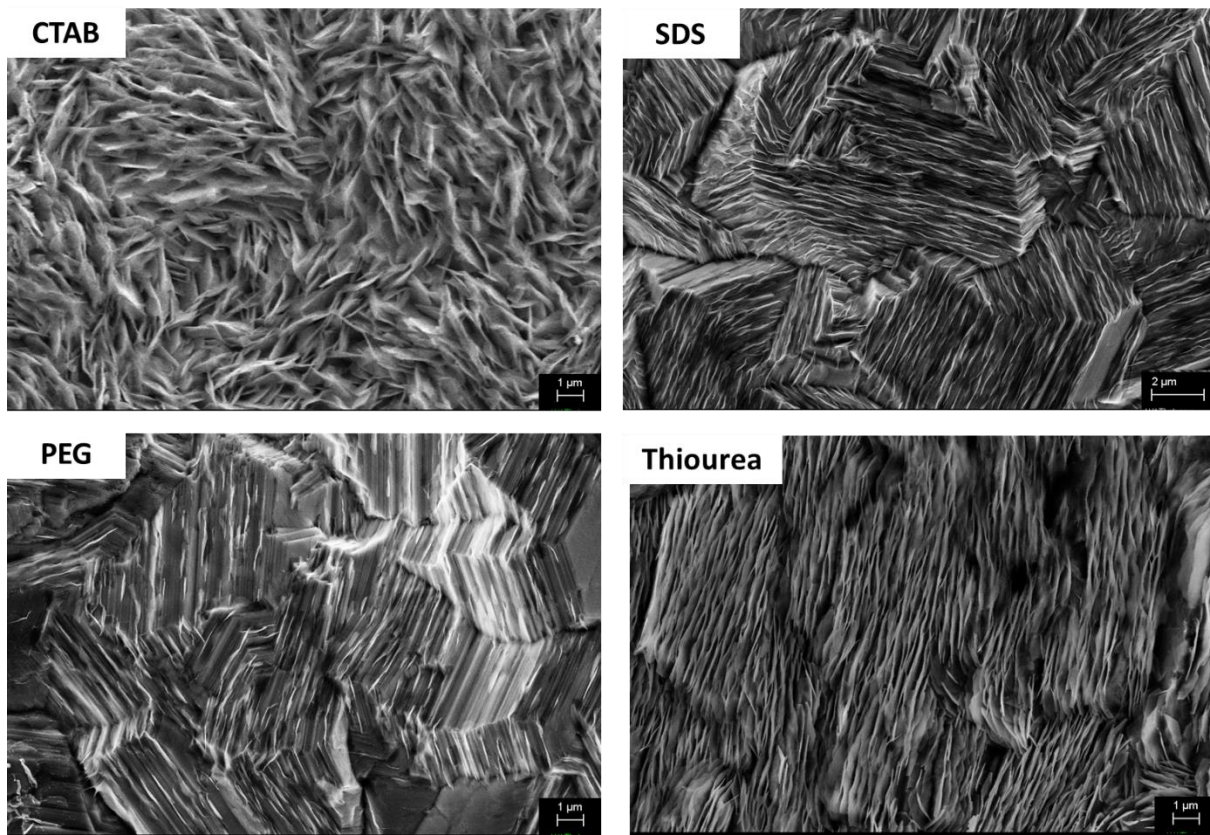
Figure 23 - SEM images of synthesized anode with organic additives (magnification 5k)

Figure 23 shows the SEM images of the electroplated zinc with the organic additives. Although the commercialized zinc foil and Zn-CTAB, Zn-SDS, and Zn-TU showed the highest (101) peak, the morphologies of the zinc were all different, which indicates that the contribution from other peaks were also important.

The morphology of Zn-CTAB was porous needle-like crystals with uniform size distributed evenly. This kind of structure was obtained due to a strong blocking effect of CTAB that increased the competition between the nucleation and crystal growth [53].

As for Zn-SDS and Zn-PEG, their morphologies were regular and uniformly distributed. The zinc deposits were growing perpendicular to the substrate and in various directions. This kind of structure is obtained when the active site and nucleation rate were reduced as additives adsorbed onto the surface of a substrate [53, 76].

As for Zn-TU, the deposit was also uniform and regular, but was not compact as Zn-SDS and Zn-PEG. Some of the area were empty possibility due to the hydrogen gas presented on the surface, blocking the zinc deposition.

3.3.5.3 Float Current
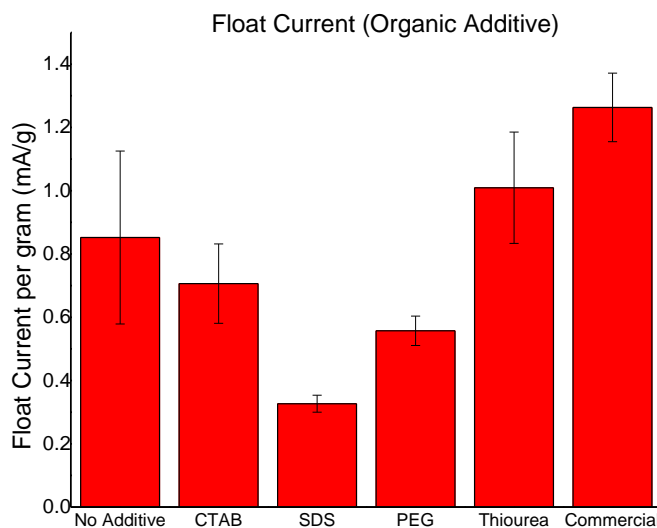
Figure 24 - Float current of ReHAB with zinc deposited with/without organic additives and commercialized zinc foil

Figure 24 is the plot of float current of ReHAB with the synthesized zinc with and without the organic additives and the commercialized zinc foil (labelled as 'Commercial'). The lowest and the highest float currents were obtained with Zn-SDS and Zn-TU, respectively. Hence, when zinc was synthesized in the bath containing SDS, Zn-SDS was able to reduce the self-discharge of ReHAB. In other words, the side reactions, or hydrogen evolution, were slowed down with Zn-SDS anode. The next lowest float current was observed from ReHAB with Zn-PEG anode.

ReHAB with Zn-CTAB produced higher float current than that with Zn-PEG due to higher surface area; but it was lower than that with Zn-TU. The float current from ReHAB with Zn-TU anode was about the same as that with the commercialized zinc foil. Moreover, the float current of the battery with Zn-No was similar to that with Zn-CTAB and Zn-TU as the error bars overlap each other. Hence, the usage of CTAB and thiourea to modify the structure of zinc was not as effective as SDS and PEG in reducing the self-discharge of ReHAB.

3.3.5.4 Corrosion Analysis

Table 4 *- Corrosion potential and current for the synthesized zinc with and without organic additives and commercialized zinc foil*

	Corrosion Potential (mV)	Corrosion Current (uA)
No Additive	-1429 ± 5	1136 ± 82
CTAB	-1431 ± 2	220 ± 7
SDS	-1431 ± 5	75 ± 14
PEG	-1422 ± 8	163 ± 32
Thiourea	-1423 ± 8	43 ± 7
Commercial	-1433 ± 2	1422 ± 110

The corrosion potential and the currents of the synthesized zinc with the organic additives are tabulated in **Table 4**. The corrosion current, or the corrosion rate, can be correlated with the float current data as both the float current and the corrosion rate are measures of zinc oxidation that mimic different states of the battery.

Both of Zn-No and the commercialized zinc foil showed relatively high corrosion current (or fast corrosion rate). As explained above, this may be due to the modified structure of the samples. The XRD data of Zn-No revealed that two highest intensities were (103) and (101), and the commercialized zinc foil (101) and (103). Thus, having two strongest peak of (103) and (101) may be the reason behind high corrosion rate.

Based on the corrosion data, the corrosion current was increased in the order of Zn-SDS, Zn-PEG, and Zn-CTAB. Thus, the corrosion rates followed the same increasing trend as the float current results (Zn-CTAB> Zn-SDS> Zn-PEG). Among the three samples, the highest corrosion was observed from Zn-CTAB. This result was expected due to the increased surface area, shown in the SEM images, as corrosion rate of a surface is proportional to its surface area.

As for Zn-TU anode, it showed the smallest corrosion current and highest float current. In other words, the anode could not solve the problem of hydrogen evolution when the battery was at the charged state (in the float current experiment), but it was able to reduce the corrosion rate. K. Song *et al.* [70] determined that thiourea has the ability to inhibit hydrogen evolution reaction, and enhance the deposition of hydrogen with zinc during zinc deposition. The authors determined that thiourea promoted zinc and hydrogen deposition between the molar ratio (H/Zn) of 0.48 to 0.84,

depending on the concentration of thiourea added to the electroplating bath [70]. According to their theory, the absorbed hydrogen either desorbed back by forming hydrogen gas or adsorbed into the deposits. Therefore, small corrosion rate of Zn-TU may be explained with smaller amount of zinc deposited in comparison to other samples, and high float current with higher amount of adsorbed hydrogen in the deposits desorbing out and forming hydrogen gas inside ReHAB.

3.3.5.5 Battery Performance
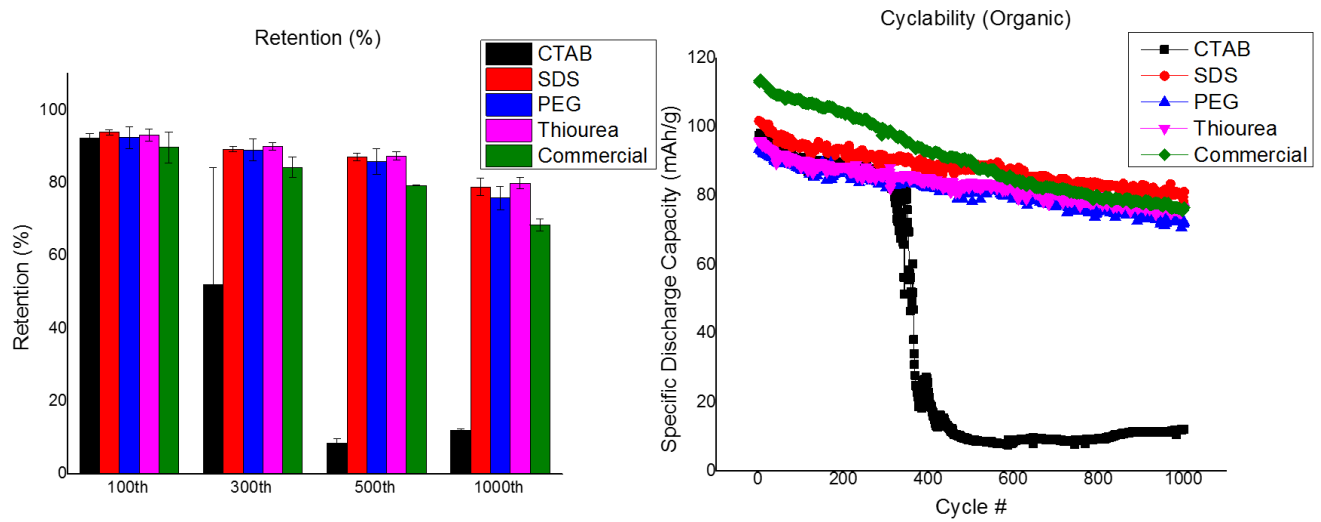
Figure 25 - Retention and cyclability of the ReHAB with zinc anode with organic additives and commercialized zinc foil

After the above experiments, ReHAB were assembled with the synthesized zinc, and their performance is summarized in **Figure 25**. All the batteries, except for the ones with Zn-CTAB, showed improved cyclaiblity. The average capacity retentions of 79, 76, 80, and 71% were obtained at the 1000th cycle from the batteries with Zn-SDS, Zn-PEG, Zn-TU, and commercialized zinc foil, respectively. Although the initial capacities of ReHAB with the electroplated zinc with the additives were lower than those with the commercialized zinc, the capacities of the batteries were more stable throughout the cycles.

As for the batteries with Zn-CTAB, a sudden capacity drop occurred after running about 350 cycles, which may be the result of the dendrites. The high surface area of Zn-CTAB possibly increased

47

the chance of the dendrites to grow, and led to the failure of the batteries. At the 1000th cycle, only 12% of original capacity was remained.

Therefore, except for Zn-CTAB, all the electroplated samples were able to solve the problems associated with the commercialised zinc foil by reducing the float current and the corrosion rate. Among the organic additives, SDS was the most preferred as it reduced the side reactions (float current and corrosion) and the capacity of the battery was well maintained until the 1000th cycle.

3.3.6 Effect of Inorganic Additives

Not many studies have been done to investigate the effect of inorganic additives during the synthesis of zinc deposits via electroplating. Hence, in this project, three inorganic additives were selected to learn how they affect on the zinc deposits. The selected inorganic additives were: indium sulfate, tin oxide, and boric acid.

Indium sulfate and tin oxide are usually used as the additives in the zinc powder anode, and their effects are determined to be:

1. Indium sulfate: inhibition of dendrite formation[77], improvement in cycle life [77]
2. Tin Oxide: suppression of hydrogen evolution [78], and stability of the electrode [79]

Unlike the above two, some of the studied presented the effects of boric acid during electroplating metal ions. Boric acid are usually used as a buffer reagent to keep the pH of the electroplating solution relatively constant. It is also used to act as a catalyst, suppress hydrogen evolution, accelerate the growth rate, and reduce the passive film during nickel electrodeposition [80].

3.3.6.1 XRD Result

XRD (Inorganic Additives)
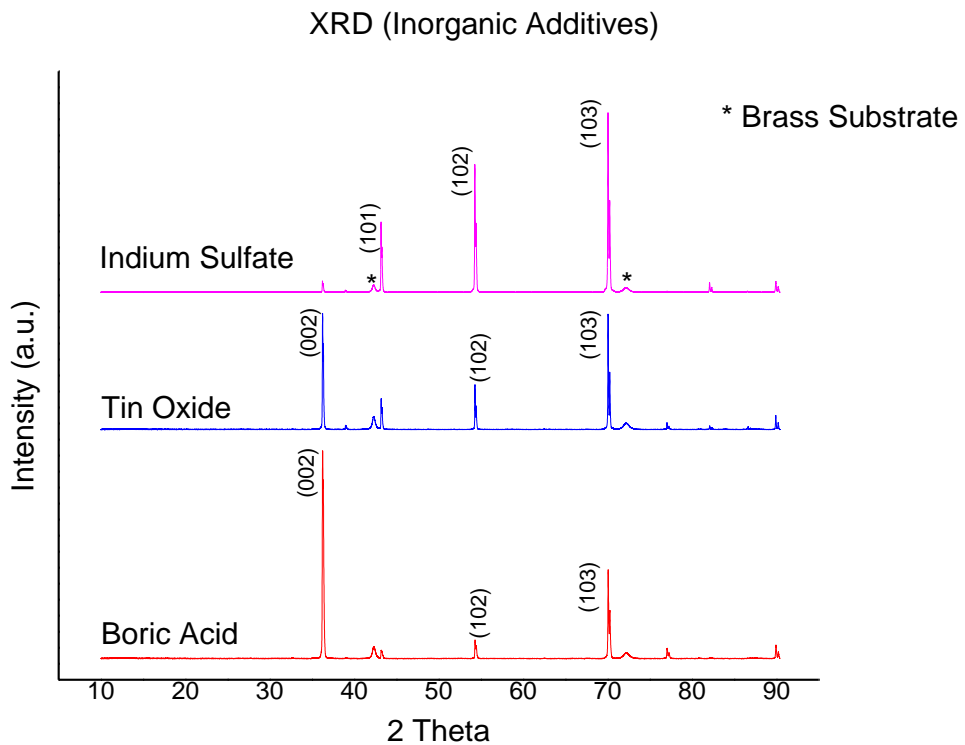
Figure 26 - XRD results of the zinc anode electroplated with inorganic additives

The crystalline structures of the zinc deposited with the inorganic additives are shown in **Figure 26**. From **Figure 26**, it can be seen that the samples electroplated with additives showed the same peak position as the zinc deposited without any additives (Zn-No) and the commercialized zinc foil. The intensities of the peak, however, were not the same as the reference zinc samples (Zn-No and the commercialized zinc foil).

Based on the XRD data, it can be seen that unlike the organic additives, it was not clear how the inorganic additives were modifying the zinc crystallinity. When indium sulfate, tin oxide, and boric acid were used to deposit zinc ions (Zn-In, Zn-TO, Zn-BA), the preferred growth orientation for Zn-In was (103), Zn-TO (002) and (103), and Zn-BA (002). Some of the data are in accordance with literature [75]. The variation in the peak intensities between literature and the obtained data may be due to the different experimental procedures [53]. As for indium sulfate, even though it promoted (103) peaks as Zn-No anode, the intensities of other peaks were different from those seen in Zn-No.

D.J. Mackinnon *et al.* [74] explained that high intensities in (002) and/or (103) planes represent the decrease in zinc deposition current efficiency. Since all samples showed dominant (002) and/or (103) planes, it can be assumed that significant amount of side reaction (hydrogen gas) occurred during the zinc deposition.

One of the interesting results is that the relative intensities of (101), (102), and (103) peaks from the three samples displayed the same trend. For instance, the XRD peaks of Zn-In presented the smallest intensity at (101) and the highest intensity at (103) among three peaks. This trend was also seen in the XRD of Zn-TO and Zn-BA. If there were no changes in (002) peak intensity, three electroplated zinc would be identical to one another. As a result, (002) planes could be one of the factors affecting the behaviour of the synthesized zinc with the inorganic additives. The smallest intensity of (002) was found in Zn-In, and the highest in Zn-BA.

3.3.6.2 SEM Result
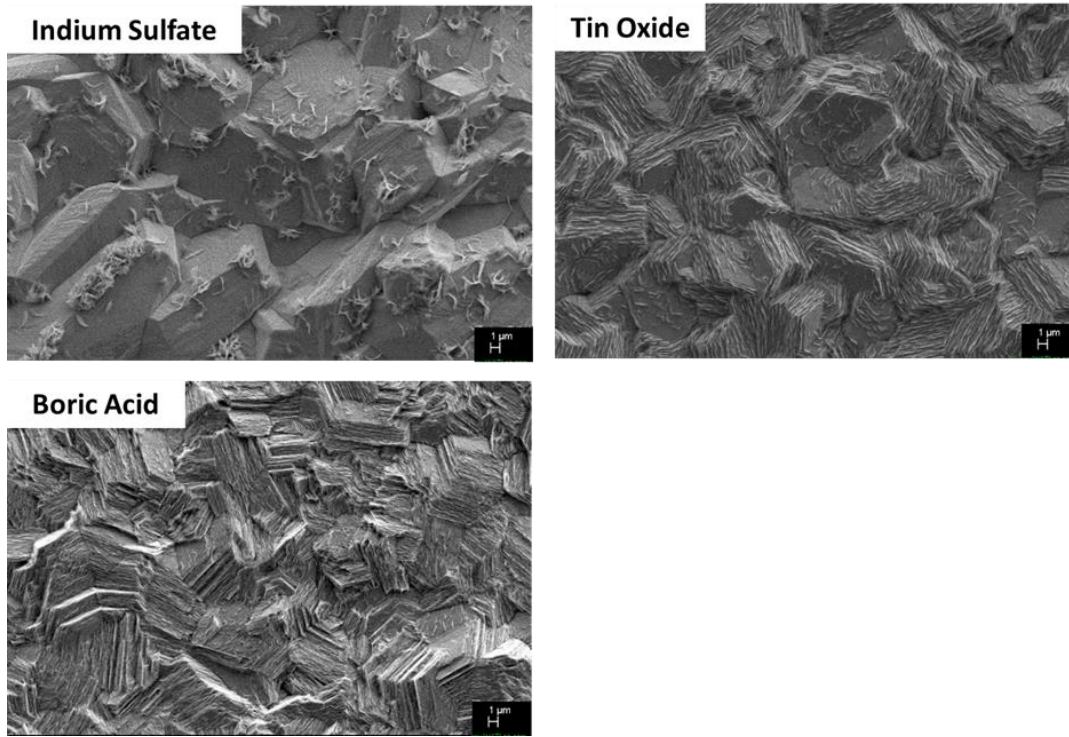
Figure 27 - SEM images of synthesized anode with inorganic additives (magnification 2k)

The morphologies of the zinc electroplated with the inorganic additives are shown in **Figure 27**. From Zn-In SEM images, a thick chunk of zinc was deposited irregularly. Each of the chunk

consisted of many layers of zinc. On top of the surface, thin fiber-like deposits were observed, which was also determined to be zinc based on the EDX analysis. This kind of morphology may be created when additives promoted (103), (102), and (101) planes and inhibited (002) planes.

As for Zn-TO and Zn-BA anodes, the morphology of the samples were similar to that of Zn-SDS and Zn-PEG. As shown in **Figure 27**, stacks of poorly defined hexagonal platelets of zinc were observed. A difference between the two samples is that the growth of zinc in Zn-TO was more organized than that in Zn-BA, because the platelets were more uniform and stacked well in Zn-TO than those in Zn-BA. More organized structure may be achieved when the intensity of (002) plane is equal to that of (103) planes (Zn-TO deposits). If the intensity of (002) planes is higher than that of (103), the size of the deposits may start to show inconsistency.

3.3.6.3 Float Current
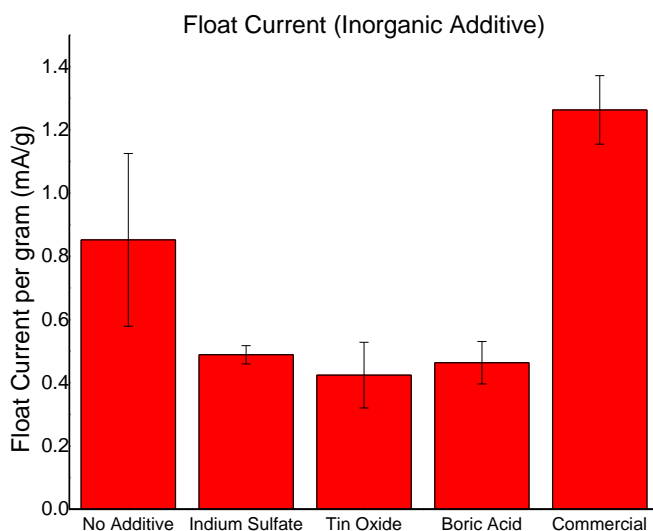
Figure 28 - Float current of ReHAB with zinc deposited with inorganic additives and commercialized zinc foil

The float current results are shown in **Figure 28**. The average float currents for ReHAB with Zn-In, Zn-TO, and Zn-BA were about twice smaller than that with Zn-No ('No Additive') and the commercialized zinc foil ('Commercial'). This indicates that if the batteries were not in use, the amount of side reactions could be reduced by the employment of Zn-In, Zn-TO, and Zn-BA. Hence,

the modified crystalline structures of the zinc with the inorganic additives were effective in suppressing hydrogen gas evolution.

3.3.6.4 Corrosion Analysis

Table 5 - Corrosion potential and current for the synthesized zinc with inorganic additives and commercialized zinc foil

	Corrosion Potential (mV)	Corrosion Current (uA)
Indium Sulfate	-1424 ± 5	120 ± 38
Tin Oxide	-1427 ± 5	125 ± 30
Boric Acid	-1419 ± 9	157 ± 12
Commercial	-1433 ± 2	1422 ± 110

As expected from the float current results, the corrosion rates of Zn-In, Zn-TO, and Zn-BA were much lower than those of Zn-No and the commercialized zinc foil. Again, the values of the corrosion rates between the synthesized samples were similar to each other. Hence, the modified anodes electroplated with these inorganic additives were effective in reducing the corrosion rates.

3.3.6.5 Battery Performance
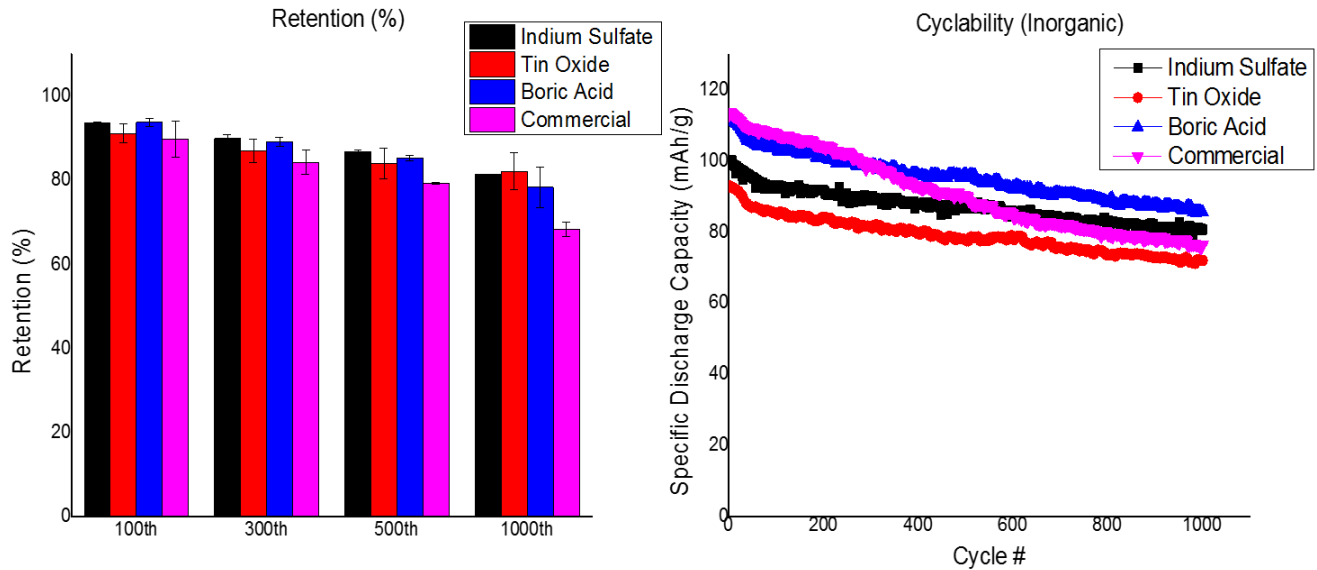
Figure 29 - Retention and cyclability of the ReHAB with zinc anode with inorganic additives and commercialized zinc foil

The performance of the synthesized zinc with the inorganic additives is shown in **Figure 29**. Similar to the batteries with zinc-organic additive anodes, better performance was observed with the ReHAB with Zn-In, Zn-TO, and Zn-BA than that with the commercialized zinc foil. At the end of 1000th cycle, the average capacity retention of 75, 82, and 78% were obtained from Zn-In, Zn-TO, and Zn-BA batteries, respectively. The batteries with Zn-In and Zn-TO showed good performance, but their initial capacities were lower than those with the commercialized zinc foil. The initial capacity of ReHAB with Zn-BA, on the other hand, was as high as the one with the commercialized zinc foil.

3.4 Conclusion

The current commercialized zinc foil raises a few problems in aqueous batteries, such as corrosion dendrite formation, and hydrogen evolution. Hence, the objective of the project was to minimize these problems by introducing a novel zinc anode synthesized by electroplating with additives.

Before the synthesis of the zinc anode with the additives, the electroplating condition was determined to deposit the minimum amount of zinc that can function well as the commercialized zinc in ReHAB. Based on the experiments, the current density of $50mA/cm^2$ and the deposition time of 10min were selected to produce zinc anodes with 100ppm of organic and inorganic additives. The zinc ions were deposited on a brass foil, treated with 25 vol. % nitric acid, as it provided a good contact between the deposits and the brass foil.

All of the anodes synthesized with additives solved the problems associated with the current zinc foil in ReHAB. When the zinc was deposited without any additives, the preferred orientation was (103). By employing CTAB, SDS, and thiourea, the plane growth changed from (103) to (101). Among the organic additives, Zn-SDS showed the lowest float current – in other words, it was able to hinder the side reactions most effectively. All of the zinc showed smaller corrosion rates than Zn-No and the commercialized zinc. When these anodes were used in ReHAB, 79, 76, and 80 % of the capacities retained after 1000th cycle with Zn-SDS, Zn-PEG, and Zn-TU, respectively. These values were much higher than that of the commercialized zinc (capacity retention at the 1000th cycle was 71%).

As for the inorganic additives, the XRD results indicated that the zinc deposition was carried out with low current efficiency as (002) and/or (103) peaks were dominant in all three samples. There was, however, no quantitative results to distinguish which of the additives generated more side reactions (or hydrogen evolution) during the zinc deposition. From the float current and corrosion results, all of the zinc anodes with the inorganic additives reduced the side reactions. When these anodes were utilized in ReHAB, 75, 82, and 78% of capacity were remained in Zn-In, Zn-TO, and Zn-BA batteries, respectively, after running 1000 cycles.

Therefore, both the organic and inorganic additives were able to solve the problems ReHAB currently faces. Despite similar performances in the float current, corrosion and the cyclaiblity tests, the organic additives may be preferred over the inorganic due to their differences in XRD

results: according to literatures, higher zinc deposition current efficiency was achieved with the organic additives. Therefore, among the four organic additives, SDS seemed the most effective additive to synthesize the 2nd generation zinc anode for ReHAB.

Chapter 4. Future Work

1. Measure voltammetry of the zinc electroplated with additives

    Cyclic voltammetry can provide detailed information on how the electroplated anodes behave during a deposition and dissolution processes as in a battery. Hence, the behaviour of the modified zinc can be explained in detail.

2. Measure hydrogen gas generated from ReHAB

    The amount of hydrogen gas generated with the battery in operation can be another evidence to indicate how effective the synthesized zinc anodes are in actual battery system.

3. Characterize the anodes after operation

    The analyses of the used anodes in the ReHAB with XRD and SEM may explain how these synthesized anodes were able to maintain high battery capacities.

4. Measure current efficiency during zinc deposition process

    The electroplated zinc with the organic and inorganic additives did improve the current issues with the commercialized zinc by reducing the corrosion rate and float current, and enhancing the battery performance., Although the XRD data may indicate high or low current efficiency of the zinc deposition according to literature, a direct measurement of the current efficiency will provide more clear data on how efficient these additives are during zinc deposition.

5. Combine additives during zinc deposition to obtain synergetic effects on the deposits

    K.O. Nayana *et al.* [81] studied the effect of CTAB and ethyl vanillin (EV) during zinc deposition. The authors determined that the deposits obtained in the bath containing CTAB and EV was bright and smooth. The grain size of the deposit was also affected. By mixing both additives together, the advantages of each additive were observed. If CTAB and EV were employed individually, the size of the grain was about 70nm. When the mixture of two was used, the grain size reduced to 49nm [81]. By reducing the grain size, brighter deposit was obtained.

References

[1]   S. Shafiee and E. Topal, "When will fossil fuel reserves be diminished?," *Energy Policy,* vol. 37, pp. 181-189, 2009.

[2]   J. M. Tarascon and M. Armand, "Issues and challenges facing rechargeable lithium batteries," *Nature,* vol. 414, pp. 359 - 367, 2001.

[3]   J. Yan, J. Wang, H. Liu, Z. Bakenov, D. Gosselink, and P. Chen, "Rechargeable hybrid aqueous batteries," *Journal of Power Sources,* vol. 216, pp. 222-226, 2012.

[4]   V. S. Bagotsky, A. M. Skundin, and Y. M. Volfkovich, *Electrochemical Power Sources: Batteries, Fuel Cells, and Supercapacitors*. New Jersey: John Wiley & Sons, Inc., 2015.

[5]   T. K. A. Hoang, T. N. L. Doan, K. E. K. Sun, and P. Chen, "Corrosion Chemistry and Protection of Zinc & Zinc Alloys by Polymer-containing Materials for Potential Use in Rechargeable Aqueous Batteries," *Royal Society of Chemistry,* vol. 5, pp. 41677 - 41691, 2015.

[6]   W. Li, W. R. McKinnon, and J. R. Dahn, "Lithium Intercalation from Aqueous Solutions," *J. Electrochem. Soc.,* vol. 141, 1994.

[7]   N. Alias and A. A. Mohamad, "Advances of aqueous rechargeable lithium-ion battery: A review," *Journal of Power Sources,* vol. 274, pp. 237-251, 2015.

[8]   W. Li and J. R. Dahn, "Lithium-Ion cells with aqueous batteries," *Journal of Electrochemical Society* vol. 142, pp. 1742 - 1746, 1995.

[9]   G. J. Wang, H. P. Zhang, L. J. Fu, B. Wang, and Y. P. Wu, "Aqueous rechargeable lithium battery (ARLB) based on LiV3O8 and LiMn2O4 with good cycling performance," *Electrochemistry Communications,* vol. 9, pp. 1873 - 1876, 2007.

[10]   J.-Y. Luo, W.-J. Cui, P. He, and Y.-Y. Xia, "Raising the cycling stability of aqueous lithium-ion batteries by eliminating oxygen in the electorlyte," *Nature Chemistry,* vol. 2, pp. 760 - 765, 2010.

[11]   J.-S. Lee, S. Tai Kim, R. Cao, N.-S. Choi, M. Liu, K. T. Lee, and J. Cho, "Metal-Air Batteries with High Energy Density: Li-Air versus Zn-Air," *Advanced Energy Materials,* vol. 1, pp. 34-50, 2011.

[12]   D. Peramunage, R. Dilon, and S. Licht, "Investigation of a novel aqueous aluminum sulfur battery," *Journal of Power Sources,* vol. 45, pp. 311 - 323, 1993.

[13]   B. T. Hang, T. Watanabe, M. Eashira, S. Okada, J.-i. Yamaki, S. Hata, S.-H. Yoon, and I. Mochida, "The electrochemical properties of Fe2O3-loaded carbon electrodes for iron–air battery anodes," *Journal of Power Sources,* vol. 150, pp. 261-271, 2005.

[14]   M. Hilder, B. Winther-Jensen, and N. B. Clark, "The effect of binder and electrolyte on the performance of thin zinc-air battery," *Electrochimica Acta,* vol. 69, pp. 308-314, 2012.

[15]   A. Ait Aghzzaf, B. Rhouta, E. Rocca, A. Khalil, and J. Steinmetz, "Corrosion inhibition of zinc by calcium exchanged beidellite clay mineral: A new smart corrosion inhibitor," *Corrosion Science,* vol. 80, pp. 46 - 52, 2013.

[16]   L. Zhu and H. Zhang, "A novel method for the modification of zinc powder by ultrasonic impregnation in cerium nitrate solution," *Ultrason Sonochem,* vol. 15, pp. 393-401, Apr 2008.

[17]   A. Renuka, A. Veluchamy, N. Venkatakrishnan, S. Nathira Begum, V. R. Chidambaram, and R. Sabapathi, "Improved cycle life performance of Zn/NiOOH cells using a

stabilized zinc electrode," *Journal of Applied Electrochemistriy,* vol. 22, pp. 182 - 184, 1992.

[18] J. Kan, H. Xue, and S. Mu, "Effect of inhibitors on Zn-dendrite formation for zinc-polyaniline secondary battery," *Journal of Power Sources,* vol. 74, pp. 113 - 116, 1998.

[19] D. Kalpana, K. S. Omkumar, S. S. Kumar, and N. G. Renganathan, "A novel high power symmetric ZnO/carbon aerogel composite electrode for electrochemical supercapacitor," *Electrochimica Acta,* vol. 52, pp. 1309-1315, 2006.

[20] A. B. Company. (2014, September 20). *What is a Short Circuit?* Available: http://www.atbatt.com/batterytimes/short-circuit

[21] S.-M. Lee, Y.-J. Kim, S. W. Eom, N. S. Choi, K. W. Kim, and S. B. Cho, "Improvement in self-discharge of Zn anode by applying surface modification for Zn-air batteries with high energy density," *Journal of Power Sources,* vol. 227, pp. 177 - 184, 2013.

[22] C. W. Lee, K. Sathiyanarayanan, S. W. Eom, and M. S. Yun, "Novel alloys to improve the electrochemical behavior of zinc anodes for zincai battery," *Journal of Power Sources,* vol. 160, pp. 1436 - 1441, 2006.

[23] Y.-D. Cho and G. T.-K. Fey, "Surface treatment of zinc anodes to improve discharge capacity and suppress hydrogen gas evolution," *Journal of Power Sources,* vol. 184, pp. 610-616, 2008.

[24] M. Ghaemi, R. Amrollahi, F. Ataherian, and M. Z. Kassaee, "New advances on bipolar rechargeable alkaline manganese dioxide–zinc batteries," *Journal of Power Sources,* vol. 117, pp. 233-241, 2003.

[25] D. J. Hubbard and C. E. A. Shanahan, "Corrosion of Zinc and Steel in Dilute Aqueous Solution," *British Corrosion Journal,* vol. 8, pp. 270 - 274, 1973.

[26] S. Choopun, N. hongsith, and E. Wangrat. (2010). *Metal-Oxide Nanowires by Thermal Oxidation Reduction Technique.* Available: http://www.intechopen.com/books/nanowires/metal-oxide-nanowires-by-thermal-oxidation-reaction-technique

[27] D. A. Jones, *Principles and Prevention of Corrosion.* New York: Macmillan Publishing Company, 1992.

[28] U. o. Cambridge. *Recycling of Metals.* Available: http://www.doitpoms.ac.uk/tlplib/recycling-metals/printall.php

[29] B. Szczesniak, M. Cyrankowska, and A. Nowacki, "Corrosion kinetics of battery zinc alloys in electrolyte solutions," *Journal of Power Sources,* vol. 75, pp. 130 - 138, 1998.

[30] C. N. Panagopoulos, E. P. Georgiou, and C. Markopoulos, "Corrosion and wear of zinc in various aqueous based environments," *Corrosion Science,* vol. 70, pp. 62 - 67, 2013.

[31] J. Zhao, D. Zhou, and W. Gan, "Effects of MoO3 on secondary alkaline zinc anode," *Ionics,* vol. 21, pp. 1983 - 1988, 2015.

[32] M. Minakshi and M. Ionescu, "Anodic behavior of zinc in Zn-MnO2 battery using ERDA technique," *International Journal of Hydrogen Energy,* vol. 35, pp. 7618 - 7622, 2010.

[33] M. Bellis. (2015, September 22). *The History of Electroplating.* Available: http://inventors.about.com/od/estartinventions/a/Electroplating.htm

[34] J.-C. Hsieh, C.-C. Hu, and T.-C. Lee, "The Synergistic Effects of Additives on Improving the Electroplating of Zinc under High Current Densities," *Journal of The Electrochemical Society,* vol. 155, p. D675, 2008.

[35] F. V. Pereira, L. V. Gurgel, and L. F. Gil, "Removal of Zn2+ from aqueous single metal solutions and electroplating wastewater with wood sawdust and sugarcane bagasse

modified with EDTA dianhydride (EDTAD)," *J Hazard Mater,* vol. 176, pp. 856-63, Apr 15 2010.

[36]   N. Alias and A. A. Mohamad, "Morphology study of electrodeposited zinc from zinc sulfate solutions as anode for zinc-air and zinc-carbon batteries," *Journal of King Saud University - Engineering Sciences,* vol. 27, pp. 43-48, 2015.

[37]   C.-C. Hu and C.-Y. Chang, "Anodic stripping of zinc deposits for aqueous batteries: effects of anions, additives, current densities, and plating modes," *Materials Chemistry and Physics,* vol. 86, pp. 195 - 203, 2004.

[38]   J. Yu, L. Wang, L. Su, X. Ai, and H. Yang, "Temperature Effects on the Electrodeposition of Zinc," *Journal of The Electrochemical Society,* vol. 150, p. C19, 2003.

[39]   K. Raeissi, A. Saatchi, and M. A. Golozar, "Effect of nucleation mode on the morphology and texture of electrodeposited zinc," *Journal of Applied Electrochemistriy,* vol. 33, pp. 635 - 642, 2003.

[40]   M. CSanchez Cruz, F. Alonso, and J. M. Palacios, "Nucleation and growth of zinc electrodeposits on a polycrystalline zinc electrode in the presence of chloride ions," *Journal of Applied Electrochemistriy,* vol. 23, pp. 364 - 370, 1993.

[41]   G. Trejo, R. Ortega B., and Y. Meas V., "Nucleation and Growth of Zinc from Chloride Concentrated Solutions," *J. Electrochem. Soc.,* vol. 145, pp. 4090 - 4097, 1998.

[42]   J. Yu, Y. Chen, H. Yang, and Q. a. Huang, "The Synergistic Effects of Additives on Improving the Electroplating of Zinc under High Current Densities," *Journal of The Electrochemical Society,* vol. 146, pp. 1789 - 1793, 1999.

[43]   A. R. Despic and M. G. Pavlovic, "Deposition of zinc on foreign substrate," *Electrochemica Acta,* vol. 27, pp. 1539 - 1549, 1982.

[44]   *The Electrochemical Society Series: Modern Electroplating*. New York: John Wiley & Sons, Inc. , 1953.

[45]   K. Yanagida, T. Aoki, A. Takahashi, and T. Igarashi, "Zinc Electroplating," U.S. Patent 3954575, 1976.

[46]   M. A. Ibrahim, "Improving the throwing power of acidic zinc sulfate electroplating baths," *Journal of Chemical Technology and Biotechnology,* vol. 75, pp. 745 - 755, 2000.

[47]   R. Winand, *Modern Electroplating*, Fifth ed.: John Wiley & Sons, Inc., 2010.

[48]   M. Paunovic and M. Schlesinger, *Fundamentals of Electrochemical Deposition* 2ed. Koboken, New Jersey: John Wiley & Sons, Inc., 2006.

[49]   M. Miyake, Y. Kubo, and T. Hirato, "Hull cell tests for evaluating the effects of polyethylene amines as brighteners in the electrodeposition of aluminum from dimethylsulfone-AlCl3 baths," *Electrochimica Acta,* vol. 120, pp. 423-428, 2014.

[50]   T. M. H. SABER and A. A. E. WARRAKY, "Electrochemical and spectroscopic studies on dezincification of alpha brass," *Br. Corros. J.,* vol. 26, pp. 279 - 285, 1991.

[51]   M. Sittig, *Electroplating and Related Metal Finishing: Pollutant and Toxic Materials Control*. New Jersey, United States: Noyes Data Corporation, 1978.

[52]   J. L. Ortiz-Aparicio, Y. Meas, G. Trejo, R. Ortega, T. W. Chapman, and E. Chainet, "Effects of organic additives on zinc electrodeposition from alkaline electrolytes," *Journal of Applied Electrochemistry,* vol. 43, pp. 289-300, 2013.

[53]   A. Gomes and M. I. da Silva Pereira, "Pulsed electrodeposition of Zn in the presence of surfactants," *Electrochimica Acta,* vol. 51, pp. 1342-1350, 2006.

[54] A. Gomes and M. I. da Silva Pereira, "Zn electrodeposition in the presence of surfactants," *Electrochimica Acta,* vol. 52, pp. 863-871, 2006.

[55] L. Oniciu and L. Muresan, "Some fundamental aspects of levelling and brightening in metal electrodeposition," *Journal of Applied Electrochemistriy,* vol. 21, pp. 565 - 574, 1991.

[56] H. H. Abdel Rahman, A. H. E. Moustafa, and S. M. K. Abdel Magid, "High rate copper electrodeposition in the presence of inorganic salts," *International Journal of Electrochemical Science,* vol. 7, pp. 6959 - 6975, 2012.

[57] V. K. Nartey, L. Binder, and K. Kordesch, "Identification of organic corrosion inhibitors suitable for use in rechargeable alkaline zinc batteries," *Journal of Power Sources,* vol. 52, pp. 217 - 222, 1994.

[58] Shanmugasigamani and M. Pushpavanam, "Role of additives in bright zinc deposition from cyanide free alkaline baths," *Journal of Applied Electrochemistry,* vol. 36, pp. 315-322, 2005.

[59] J. C. Ballesteros, P. Díaz-Arista, Y. Meas, R. Ortega, and G. Trejo, "Zinc electrodeposition in the presence of polyethylene glycol 20000," *Electrochimica Acta,* vol. 52, pp. 3686-3696, 2007.

[60] J. F. Shackelford, *Introduction to Materials Science for Engineers*, 7th ed. New Jersey: Person Education, Inc. , 2009.

[61] Y. Tan, *Heterogeneous Electrode Processes and Localized Corrosion*. New Jersey: John Wiley & Sons, Inc., 2013.

[62] M. C. Li, L. L. Jiang, W. Q. Zhang, Y. H. Qian, S. Z. Luo, and J. N. Shen, "Electrodeposition of nanocrystalline zinc from acidic sulfate solution containing thiourea and benzalacetone as additives," *Journal of Solid State Electrochem,* vol. 11, pp. 549 - 553, 2007.

[63] Q. Li, W. Fu, Y. Mu, W. Zhang, P. Lv, L. Zhou, H. Yang, K. Chi, and L. Yang, "The effect of CTAB concentration on the properties of electrodeposited cadmium telluride films," *CrystEngComm,* vol. 16, p. 5227, 2014.

[64] R. K. Ghavami, Z. Rafiei, and M. Tabatabaei, "Effects of cationic CTAB and anionic SDBS surfactants on the performance of Zn–MnO2 alkaline batteries," *Journal of Power Sources,* vol. 164, pp. 934 - 946, 2007.

[65] K. O. Nayana and T. V. Venkatesha, "Bright zinc electrodeposition and study of influence of synergistic interaction of additives on coating properties," *Journal of Industrial and Engineering Chemistry,* 2014.

[66] D. J. Mackinnon, J. M. Brannen, and R. M. Morrison, "The effect of thiourea on zinc electrowinning from industrial acid sulphate electrolyte," *Journal of Applied Electrochemistriy,* vol. 18, pp. 252 - 256, 1988.

[67] N. Alias and A. A. Mohamad, "Morphology study of electrodeposited zinc from zinc sulfate solutions as anode for zinc-air and zinc-carbon batteries," *Journal of King Saud University - Engineering Sciences,* vol. 27, pp. 43-48, 2013.

[68] K. O. Nayana and T. V. Venkatesha, "Bright zinc electrodeposition and study of influence of synergistic interaction of additives on coating properties," *Journal of Industrial and Engineering Chemistry,* vol. 26, pp. 107-115, 2015.

[69] R. K. Ghavami and Z. Rafiei, "Performance improvements of alkaline batteries by studying the effects of different kinds of surfactant and different derivatives of benzene

on electrochemical properties of electrolytic zinc," *Journal of Power Sources,* vol. 162, pp. 893 - 890, 2006.

[70] K.-D. Song, K.-B. Kim, S.-H. Han, and H. Lee, "Effect of Additives on Hydrogen Evolution and Absorption during Zn Electrodeposition Investigated by EQCM," *Electrochemical and Solid-State Letters,* vol. 7, p. C20, 2004.

[71] G. Trejo, R. Ortega, and Y. Meas, "The effect of polyethylene glycol 8000 additive on the deposition mechanism & morphology of zinc deposits," *Plating and Surface Finishing,* vol. 86, pp. 84 - 87, 2002.

[72] C. A. Loto and R. T. Loto, "Effect of Dextrin and Thiourea Additives on the Zinc," *International Journal of Electrochemical Science,* vol. 8, pp. 12434 - 12340, 2013.

[73] B. C. Tripathy, S. C. Das, P. Singh, and G. T. Hefter, "Zinc electrowinning from acidic sulphate solutions. Part III: Effects of quaternary ammonium bromides," *Journal of Applied Electrochemistriy,* vol. 29, pp. 1229 - 1235, 1999.

[74] D. J. Mackinnon and P. L. Fenn, "The effect of tin on zinc electrowinning from industrial acid sulphate electrolyte," *Journal of Applied Electrochemistriy,* vol. 14, pp. 701 - 707, 1984.

[75] D. J. Mackinnon, J. M. Brannen, and H. P. Feng, " Characterization of impurity effects in zinc electrowinning from industrial acid sulphate electrolyte," *Journal of Applied Electrochemistriy,* vol. 17, pp. 1129 - 1143, 1987.

[76] G. Trejo, H. Ruiz, R. Ortega Borges, and Y. Meas, "Influence of polyethoxylated additives on zinc electrode," *Journal of Applied Electrochemistriy,* vol. 31, pp. 685 - 692, 2001.

[77] J. Daniel-Ivad, R. James Book, and K. Tomantschger, "Sealed rechargeable cells containing mercury-free zinc anodes, and a method of manufacture," US Patent, 1997.

[78] M. Tokuda, M. Yano, M. Nogami, S. Fujitani, and K. Naishio, "Sealed, alkaline-zinc storage battery," US Patent US 6265105 B1, 1998.

[79] J. Phillips, "Methods for production of zinc oxide electrodes for alkaline batteries," US7816035 B2, 2010.

[80] Y. Tsuru, M. Nomura, and F. R. Foulkes, "Effect of boric acid on hydrogen evolution and internal stress in films deposited from a nickel sulfamate bath," *Journal of Applied Electrochemistriy,* vol. 32, pp. 629 - 634, 2002.

[81] K. O. Nayana, T. V. Venkatesha, B. M. Praveen, and K. Vathsala, "Synergistic effect of additives on bright nanocrystalline zinc electrodeposition," *Journal of Applied Electrochemistry,* vol. 41, pp. 39-49, 2011.